Summer 2015

Optimal techno-economic sizing of wind/solar/battery hybrid microgrid system using the forever power method

Sami Hamed Alalwani

Department:

OPTIMAL TECHNO-ECONOMIC SIZING OF WIND/SOLAR/BATTERY HYBRID MICROGRID SYSTEM USING THE FOREVER POWER METHOD

by

SAMI HAMED ALALWANI

A THESIS

Presented to the Faculty of the Graduate School of the

MISSOURI UNIVERSITY OF SCIENCE AND TECHNOLOGY

In Partial Fulfillment of the Requirements for the Degree

MASTER OF SCIENCE IN ELECTRICAL ENGINEERING

2015

Approved by

Dr. Jonathan W. Kimball, Advisor
Dr. Mehdi Ferdowsi
Dr. Pourya Shamsi

ABSTRACT

Advancement in power electronics, energy storage, control, and renewable energy sources has led to the use of integrated renewable energy sources in islanded microgrids (MG). Also, the uses of integrated renewable energy sources have become more technically applicable, more economically feasible, and more environmentally friendly than conventional sources. As a result, electrification of rural villages using renewable energy technologies has started to become widely adopted around the world. Since generating power from renewable energy sources is highly intermittent and difficult to predict, the use of proper energy storage technology is important to eliminate mismatches between the load demand and generation. Obtaining proper unit sizing for energy sources and storage is critical in determining the cost and reliability of the system. It is challenging to properly optimize the size of hybrid micro-sources for islanded MGs with minimum capital and operational cost while still achieving the targeted availability of the power supply. In this research, typical meteorological data is used with the Forever Power method to generate all possible combinations of PV modules and wind turbines along with the corresponding availability of the power supply. The goal of the study is to allow the designer of the system to select the size that best fits the targeted availability of the power supply with the most economical cost. As a case study, this method has been applied to an isolated MG for four homes in a rural area outside of Yanbu City, Saudi Arabia. A techno-economic analysis was applied using MATLAB to find the optimal size of the hybrid micro-sources.

ACKNOWLEDGMENTS

First and foremost, I would like to express gratitude and appreciation to Dr.Jonathan Kimball, my advisor throughout my Master's program. He provided me with incredible guidance and provided me with great knowledge throughout my time at Missouri University of Science and Technology. I would also like to thank Dr. Mehdi Ferdowsi and Dr. Pourya Shamsi, two committee members for my thesis.

Also, I would like to give my sincere gratitude to the Royal Commission of Yanbu Colleges and Institutes (RCYCI) for providing me with a full scholarship to pursue my higher education and obtain my Master's degree at one of the most prestigious universities in the United States. I am very thankful for H.E. Dr. Alaa Nassif, the Executive President of the Royal Commission of Yanbu for his approval to build a partnership with the Office of Sustainable Energy and Environmental Engagement at Missouri University of S&T to design and build the Yanbu Solar Village. Also, I would like to thank Dr. Ahmed Dabroom, the Managing Director of RCYCI, for his support throughout my career and academic journey.

Finally, I am deeply grateful to my mother and wife for their patience and support throughout my studies. I would like to dedicate this thesis to my brother, Ibrahim Alalwani, and my cousins, Ghazi and Mohammed Alalwani.

TABLE OF CONTENTS

LIST OF ILLUSTRATIONS

Figure Page

LIST OF TABLES

1. INTRODUCTION

The energy demand in the Kingdom of Saudi Arabia has increased dramatically in response to significant industrial, commercial, and residential developments. According to BP Statistical Review of World Energy 2014, the total electrical energy generated in 2013 was 292.2 TWh, approximately 7% more than the electrical energy generated in 2000 [1]. The generation capacity in the kingdom is about 58 GW with all plants being powered by either oil or natural gas as shown in Figure 1.1 [2] [3]. Figure 1.2 shows the generation capacity based on the type of energy source used by Saudi Electricity Company (SEC) [4].

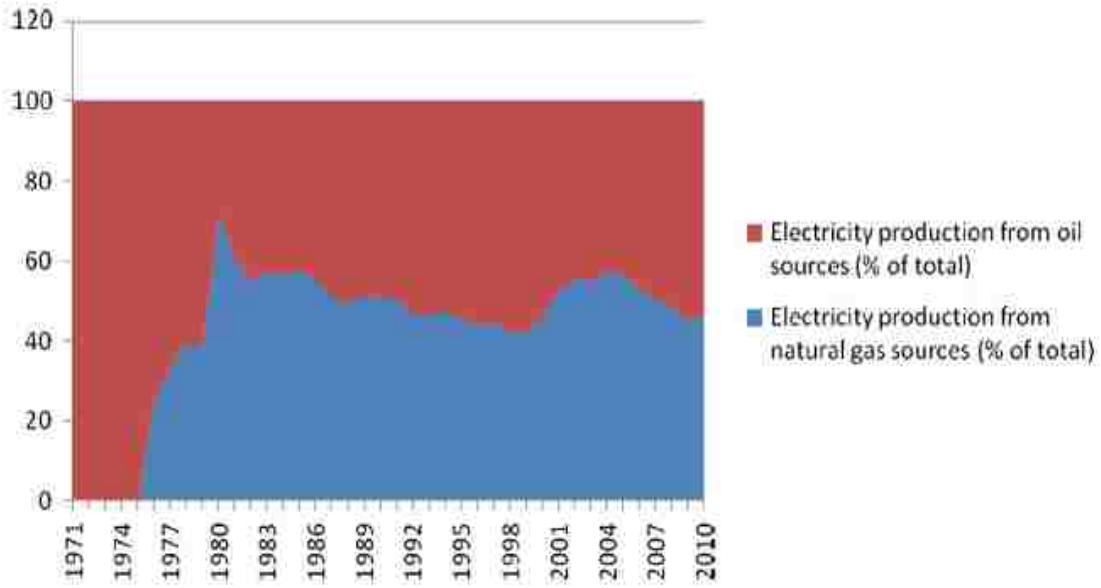

Figure 1.1 Percentage of electricity production by type of fuel [3]

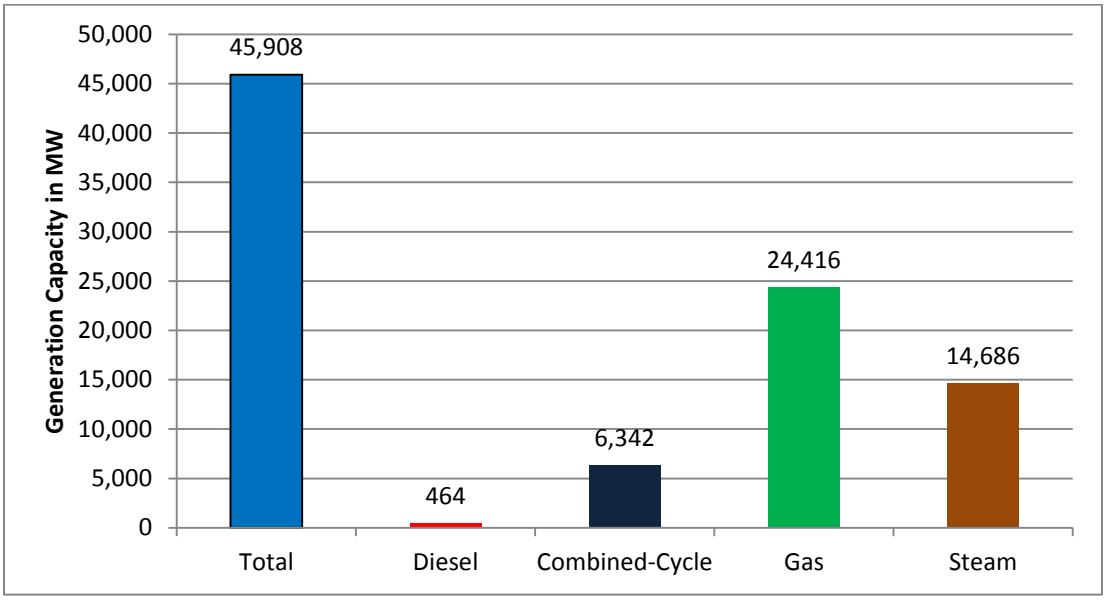

Figure 1.2 Power generation capacity per type of generation, 2013 [4]

By 2032, the power generation capacity is forecast to be 120 GW [5]. Electricity consumption per capita has increased at an annual rate of 6.5% between 2000 and 2008 [6]. According to a Saudi Arabia energy efficiency report, the electricity consumption per capita in 2010 was approximately 8300 kWh/cap. The US average at this time was 13,395 kWh [7]. Recently, Saudi Arabia has devoted significant attention and resources to the diversification of energy and has incorporated renewable energy technologies. As a result, oil and gas exports, two items which account for approximately 90% of the country's revenue, have not been impacted by domestic consumption (Figure 1.3).

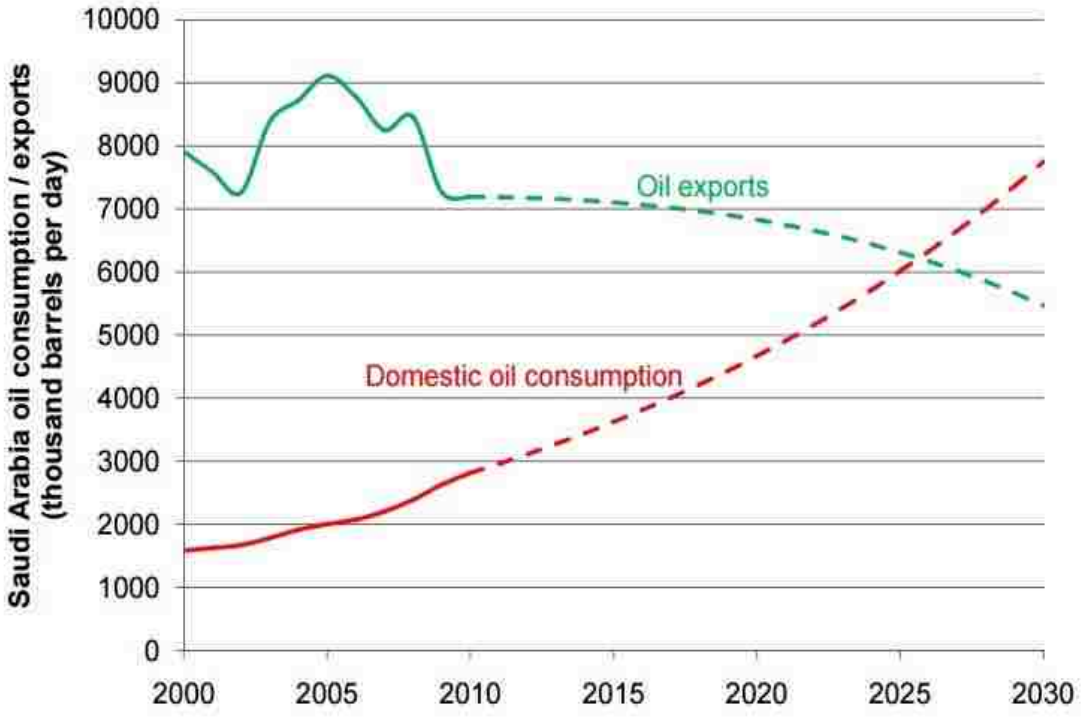

Figure 1.3 Projection of domestic oil consumption in Saudi Arabia [10].

Government of Saudi Arabia provides consumption subsidies to electrical energy producers to sell power below cost. In 2013, the total electrical energy subsidy by the government was approximately $40 billion. In the same year, the average cost of kWh sold by the SEC was 3.76 cents/kWh. Without the government subsidies, the cost would have been 21.33 cents/ kWh [10].

Saudi Arabia has two main seasons, winter and summer. The peak power demand during summer is much higher than in winter due to heavy air conditioning use as illustrated by Figure 1.4. In addition, winter in Saudi Arabia is relatively mild and very few heaters need to be used.

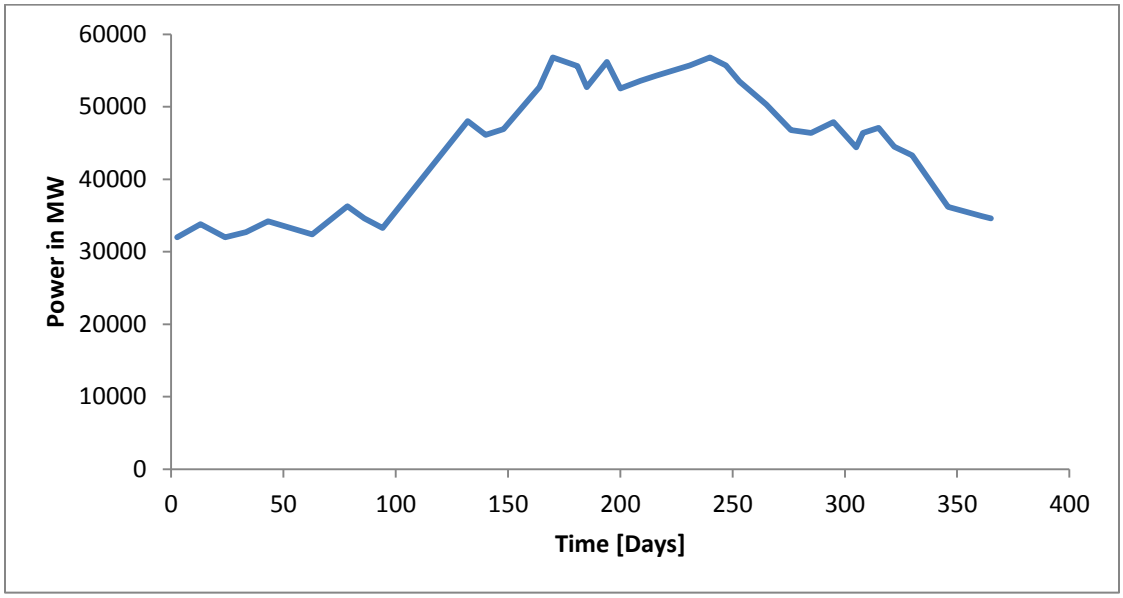

Figure 1.4 Load variation in Saudi Arabia, 2013 [8].

In 2011, King Abdullah launched the King Abdullah City for Atomic and Renewable Energy (KA-CARE) to prepare a strategic plan for Saudi Arabia's energy supply. The suggested plan by KA-CARE involves attaining a photovoltaic solar panel with a capacity of 16 GWp by 2032 [11]. Because of its geography, Saudi Arabia possesses great solar energy potential and has the ability to produce this energy at a low cost. An analysis performed by Clear Sky advisors in Saudi Arabia showed that the price of electricity generated by a large scale solar PV system is about $0.15/kWh compared to $0.127-$0.174/kWh for electricity generated by conventional power plants [13]. Saudi Arabia has an area of approximately 2.2 millions square kilometers, most of which are unpopulated. However, there are many remote villages scattered throughout the kingdom which have no access to the utility grid. These villages depend entirely on diesel

generators as their main source of electricity. These isolated villages have a total power generation capacity of 2.489 GW [4].

There are many disadvantages associated with using diesel generators including high maintenance and operational costs. In addition, competitive technologies such as solar and wind generators (WGs) are becoming viable energy sources. These technologies can be used with either diesel generators to maximize performance and reduce the total cost of producing energy or can be hybridized with an appropriate energy storage technology.

1.1 GLOBAL SOLAR RADIATION IN SAUDI ARABIA

Rehman et al. found that the average global solar radiation in Saudi Arabia varied between a minimum of 1.63 MWh/m^2 yr and a maximum of 2.65 MWh/m^2-yr at Tabuk and Bisha, respectively [14]. As shown in Figure 1.6 and 1.7, Saudi Arabia receives high solar radiation intensity and has many hours of intense sunlight [14] [15]. The average daily global solar insolation in the Kingdom of Saudi Arabia is high and exceeds 6 kWh/m^2-day from April to September. Figure 1.6 illustrates how this high solar insolation coincides with high load demand during these months. As a result, solar energy can be utilized for peak load sharing for the national grid. Rehman et al. also found that the average sunshine duration across 41 locations in Saudi Arabia was 8.89 hours per day and that the mean value of the specific yield was 260.83 kWh/m^2 [14].

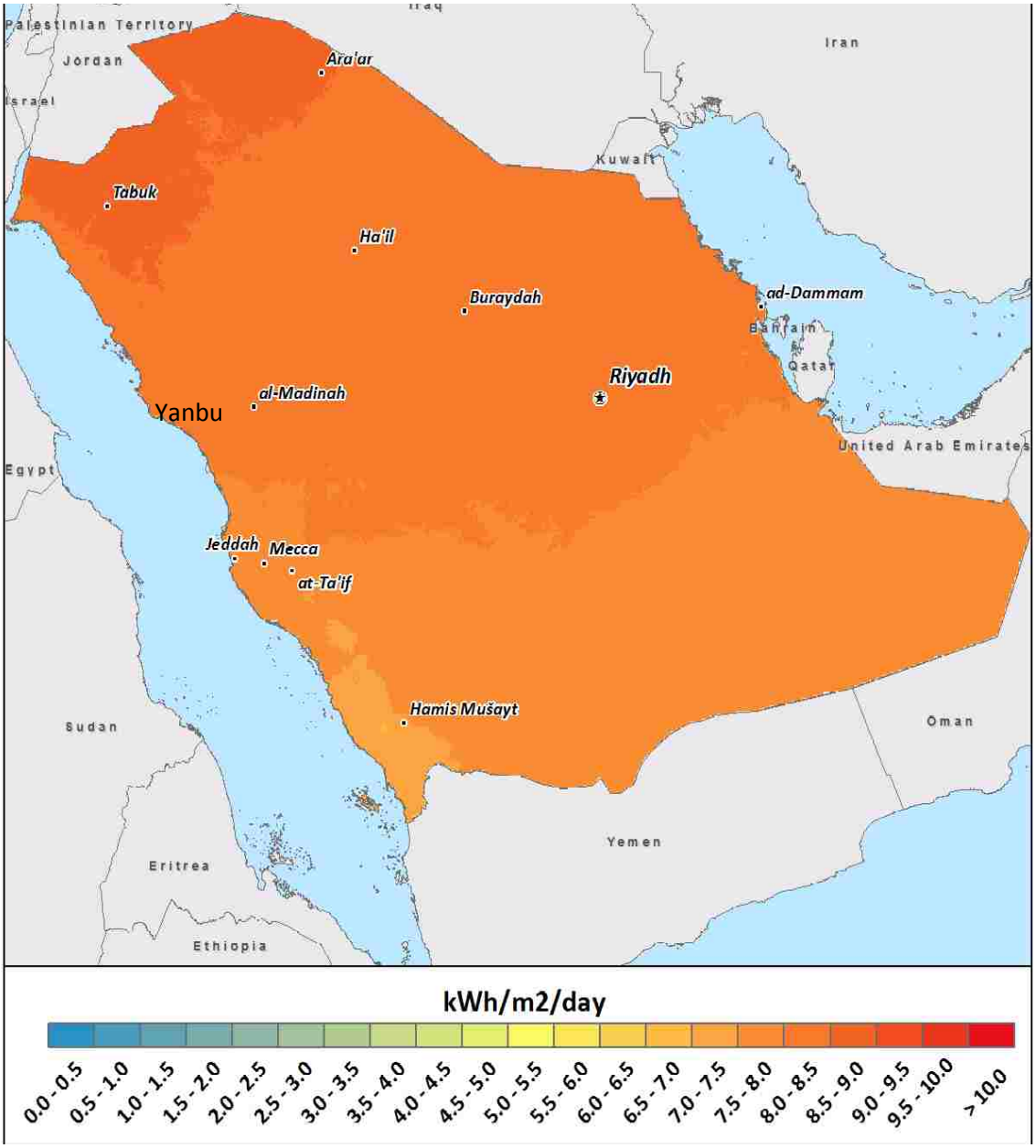

Figure 1.5 Average Daily Total GHI in JUNE for years 1999-2012 [16]

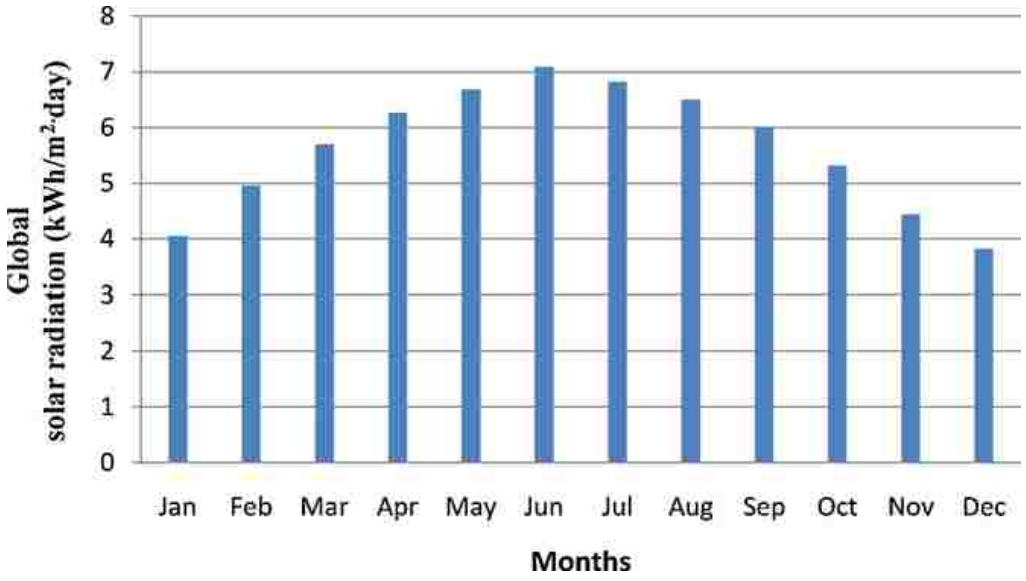

Figure 1.6 Average daily seasonal variation of global solar radiation for Saudi Arabia[14]

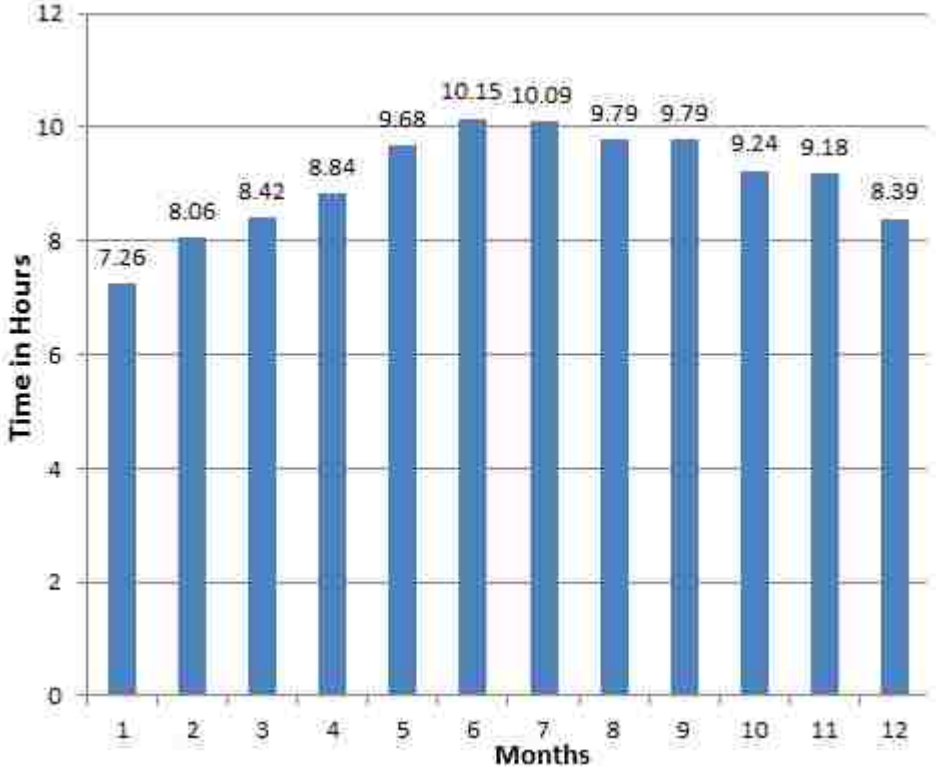

Figure 1.7 Average variation of sunshine duration over a year in Saudi Arabia [14]

1.2 SOLAR ENERGY PROJECTS IN SAUDI ARABIA

In 1977, Saudi Arabia initiated an international joint program involving the Saudi Arabian Energy Research Institute (ERI), American SOLERAS program, and the German HYSOLAR program [14]. Between 1981 and 1987, the joint program was able to design and build a solar village with a total PV generation capacity of 350 kWp that was able to generate between 1 to 1.5 MWh per day [12]. Table 1.1 shows other projects conducted by ERI using a PV energy system [17].

In 2010, there were 9300 PV modules installed on the campus of King Abdullah University of Science and Technology. The modules were able to produce a peak power of 2 MW [14]. In 2011, a 500 kWp solar power plant was constructed at Farasan Island, south of Saudi Arabia. In addition, Aramco, a Saudi oil company, constructed its headquarters in Dhahran of Saudi Arabia, the world's largest solar parking project that has a power capacity of 10 MW [15].

Table 1.1 List of solar energy projects conducted by the ERI, KACST [17]

Projects	Location	Duration	Applications
350 kW PV system	Solar Village	1981-87	AC/DC electricity for remote areas
350 kW PV hydrogen production plant	Solar Village	1987-93	Demonstration plant for solar hydrogen production
Solar cooling	Saudi universities	1981-87	Developing of solar cooling laboratory
1 kW solar hydrogen generator	Solar Village	1989-93	Hydrogen production, testing and measurement (laboratory scale)
2 kW solar hydrogen	KAU, Jeddah	1986-91	Testing of different electrode materials for solar hydrogen plant
3 kW PV test system	Solar Village	1987-90	Demonstration of climatic effects
4 kW PV system	Southern regions of Saudi Arabia	1996	AC/DC electricity for remote areas
6 kW PV system Solar seawater desalination	Solar Village	1996-98	PV grid connection
PV water desalination (0.6 m^3 per hour)	Sadous Village	1994-99	PV/RO interface
Solar-thermal desalination	Solar Village	1996-97	Solar distillation of brackish water
PV in agriculture (4 kWp)	Muzahmia	1996	AC/DC grid connected
Long-term performance of PV (3 kW)	Solar Village	Since 1990	Performance evaluation
Fuel cell development (100±1000 W)	Solar Village	1993-2000	Hydrogen utilization

1.3 SOLAR ENERGY CAPACITY AT YANBU CITY

Yanbu City is located on the Red Sea coast of Saudi Arabia (figure 1.5) and has geographic coordinates of 24° 5' 7" North, 38° 2' 55" East. It is 6 meters above sea level. Yanbu City has favorable conditions for using solar energy. Figure 1.8 shows the solar irradiance for Yanbu from 2007 to 2014. The average peak amount of sun at Yanbu lasts for approximately 6.27 hours and has an average solar irradiance of 261.4 W/m^2.

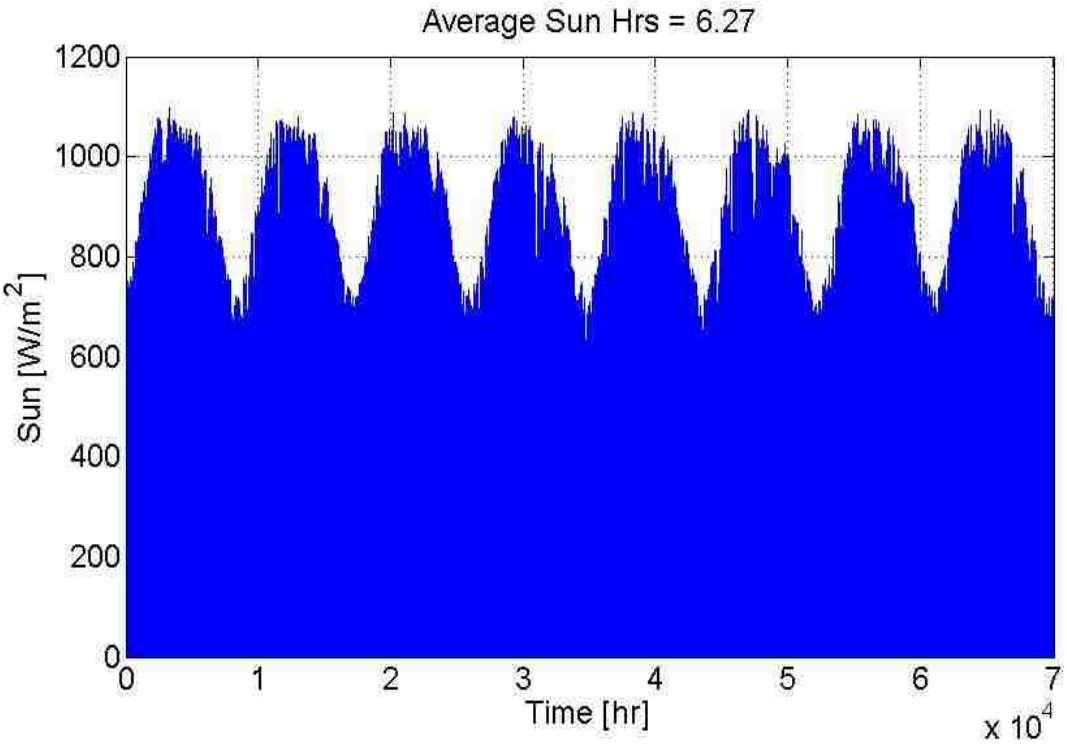

Figure 1.8 Solar irradiance at Yanbu City (2007-2014)

The long term average of the yearly sum of global horizontal irradiance (GHI) at Yanbu is 2290.9 kWh/m^2. Figure 1.9 below shows the average yearly sum of GHI from 2007 to 2014.

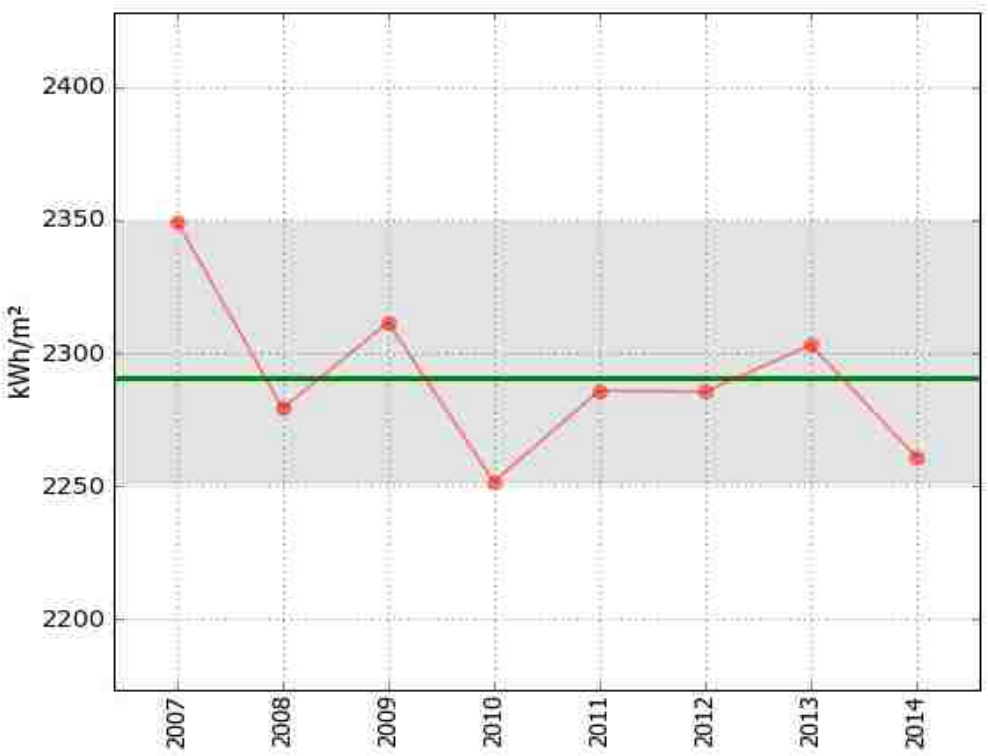

Figure 1.9 Annual variability of yearly sums of GHI at Yanbu

The long-term sum of the average monthly GHI (kWh/m^2) at Yanbu from 2007 to 2014 is shown in Figure 1.10. The figure illustrates that solar energy during summer is higher than in winter, something which coincides with trends in electricity demand. The maximum is 247.9 kWh/m^2 (July, 2010) and the minimum is 125.2 kWh/m^2 (January, 2008).

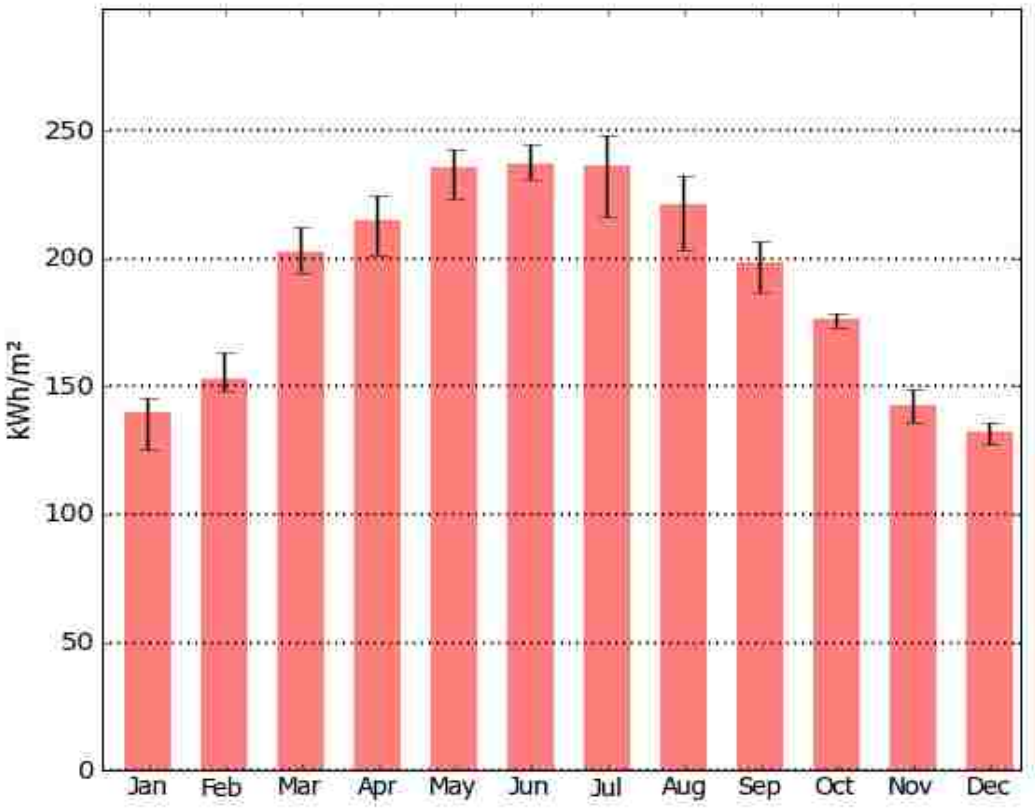

Figure 1.10 Monthly sums of GHI: long-term average, minimum and maximum

1.4 WIND ENERGY CAPACITY IN SAUDI ARABIA

Saudi Arabia is characterized by two vast coastal windy regions, namely the Arabian Gulf and the Red Sea. The annual mean wind speed in these two regions exceeds 4.63 m/s [18]. In 1970, meteorological data collection stations were installed in Saudi Arabia airports. Ansari et al. [19] developed a wind atlas in 1986 using hourly wind speed data in Saudi Arabia. To accurately assess wind energy potential, certain statistical features of wind speed must be studied. For example, the Weibull probability distribution function is used to find the monthly frequency distribution of wind speed

measurement. Also, Rehman et al. found the Weibull parameter for 10 locations in Saudi Arabia using the Weibull distribution function and used long-term wind speed data for 20 locations throughout Saudi Arabia [19] and used this data to calculate the cost of kilowatt hours of electricity produced using different wind machines [20]. The monthly and annual wind speeds and wind powers at these locations, ranged from 2.5 to 4.4 m/s^2 and from 21.8 to 77.7 W/m^2, respectively [22]. The strategic plane presented by KA-Care revealed that the cumulative wind power capacity will reach 9 GW of power by 2032 [12].

1.5 WIND CAPACITY AT YANBU CITY

According to Ansari et al., Yanbu has 86,748 recorded hours of wind speed at a height of 10 meters [19]. A wind power cost analysis conducted by Rehman at twenty locations through the kingdom of Saudi Arabia concluded that Yanbu has the highest wind potential of all areas tested [20]. According to Rehman [23], an annual energy production of 4941487.2 kWh was obtained using a 2500 kW wind turbine and achieved the lowest energy cost ($0.0234/kWh). Using meteorological data at a height of 10 meters recorded since 1970, Rehman investigated the recorded wind speeds at Yanbu during a 13-year span and showed that the yearly mean wind speed at Yanbu varied from a high of 6 m/s to a low of 3 m/s. The same study also found that the monthly mean variation of wind speed was greater than 4 m/s in all months. The mean wind speed is higher during the summer, something which coincides with a higher load trend in Yanbu. Data collected from 1970 to 1983 also showed that wind speeds between 4 and 10 m/s were measured almost 60% of the time and speeds greater than 10 m/s were measured 8% of the time [20].

Further research performed by Rehman et al. found that the development of a wind park with a capacity of a 1500 kW machine will result in a reduction of greenhouse gases by 31,369 tons per year. The same study showed that the years-to-positive cash flow (YPCF) or the return on investment for Yanbu was the lowest of the five locations in Saudi Arabia that could be made into wind farms. Yanbu had YPCF as low as 5.1 years for a 1.5 MW turbine [23]. Another study by Rehman et al. showed that the daily mean value of wind speed at Yanbu from 1990 to 2006 was 3.76 m/s with a maximum speed of 10.3 m/s [24].

In this study, Yanbu wind data from the beginning of 2007 to the end of 2014 were used. During this time, the mean wind speed was 3.72 m/s. Generally, a wind speed above 4 m/s is recommended for small scale wind turbines. Figure 1.11 below shows the annual average wind speed at Yanbu for eight consecutive years.

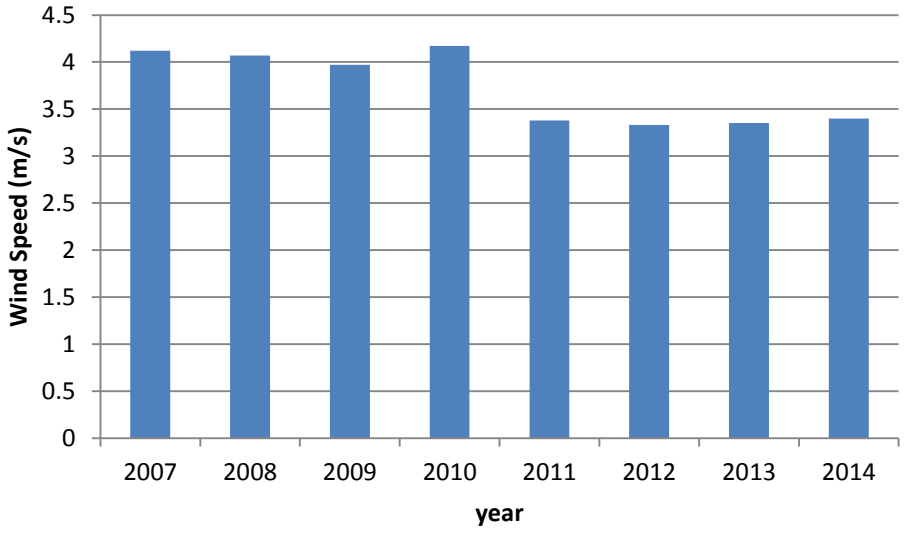

Figure 1.11 Annual average wind speed at Yanbu

The highest wind speed recorded was 11.9 m/s. Most small scale WGs require a wind speed of 3 m/s to generate power. At Yanbu, wind speeds recorded from 2007 to 2014 were greater than or equal to 3 m/s 63.13% of the time. Figure 1.12 shows the frequency distribution of wind speeds during the full period used in this study.

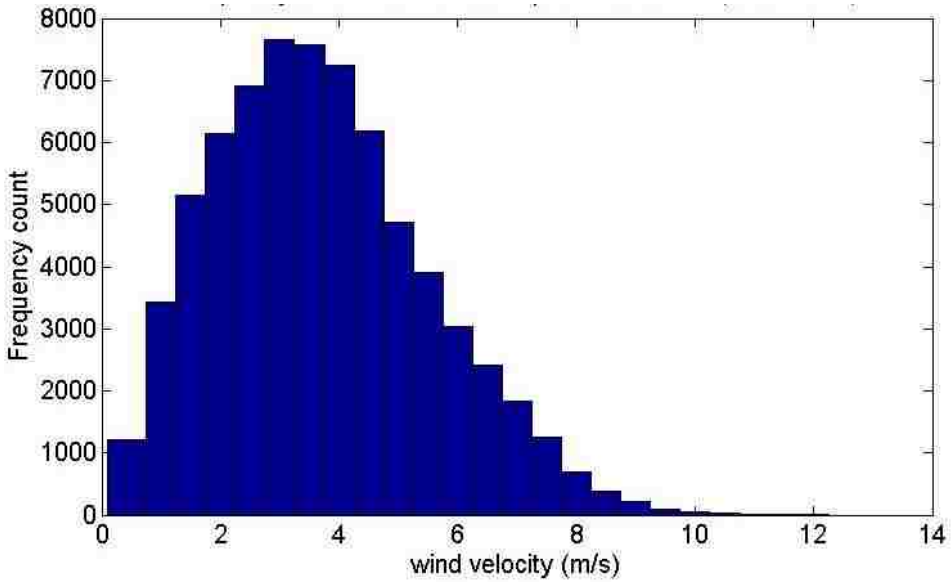

Figure 1.12 Frequency distribution of wind speeds (2007-2014)

Moreover, figure 1.13 shows that there is not much variation in wind speed throughout the year and that makes it predictable and reliable. A higher average wind speed was observed during summer for eight consecutive years which coincide with the increased electricity demand. On the other hand, lower wind speeds were observed during the winter months, a time when electricity demand is lower.

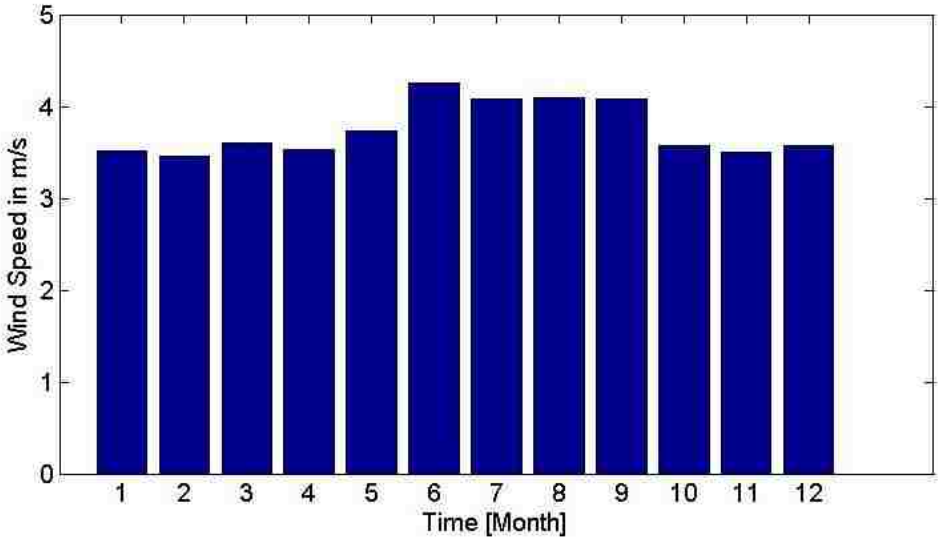

Figure 1.13 Average monthly wind speeds (2007-2014)

2. LITERATURE REVIEW

There are many rural villages in countries around the world that do not have access to electricity. According to International Energy Agency (IEA), more than 1.3 billion people around the world do not have access to electricity. Approximately 84% of these people live in rural villages [25]. Recently, because of the advancement in power electronics, renewable energy sources and energy storage technologies have allowed the cost of led the cost of energy from renewable resources to compete with conventional resources. One of the existing solutions to electrify rural villages is the use of MG energy systems. An MG can be defined as a group of interconnected loads and distributed energy resources within clearly defined electrical boundaries. These resources act as a single controllable entity that connects or disconnects from the grid to enable it to operate in a grid-connected or "island" mode [26] [27]. The hybridization and integration of renewable energy resources for an MG are used to obtain optimal control and energy management. Figure 2.1 shows a block diagram for a MG energy system [28].

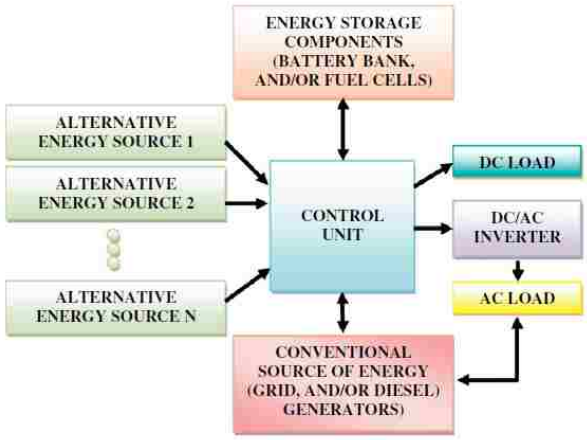

Figure 2.1 General structure of a microgrid system [28]

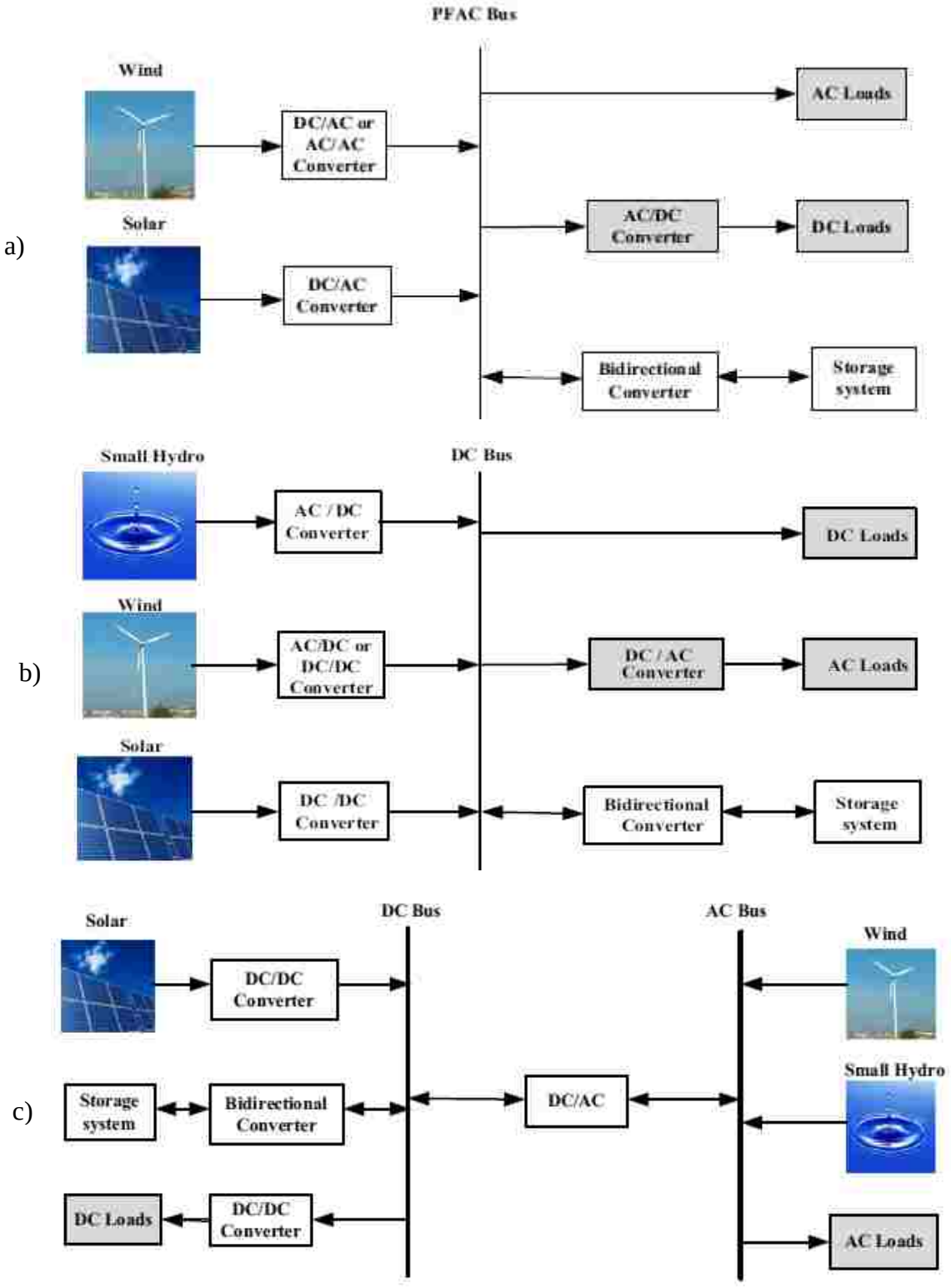

Figure 2.2 Microgrid configurations: a) AC coupled b) DC coupled c) Hybrid coupled [29]

Integration configurations between different energy sources and loads in an MG can be categorized into three possible configurations: AC coupled, DC coupled, and hybrid coupled configuration as shown in Figure 2.2 [29]. Each configuration has its own advantages and disadvantages in terms of control complexity, cost, efficiency and reliability.

Unit sizing of photovoltaic (PV) panels and wind turbines with energy storage for an islanded MG has been studied by many researchers. The criteria for choosing the optimal size of integrated renewable energy system (IRES) are usually influenced by economic and power reliability factors. There are many methodologies applied to proper unit sizing of an isolated hybrid PV-wind MG system which can be summarized as shown in Figure 2.3 below [29].

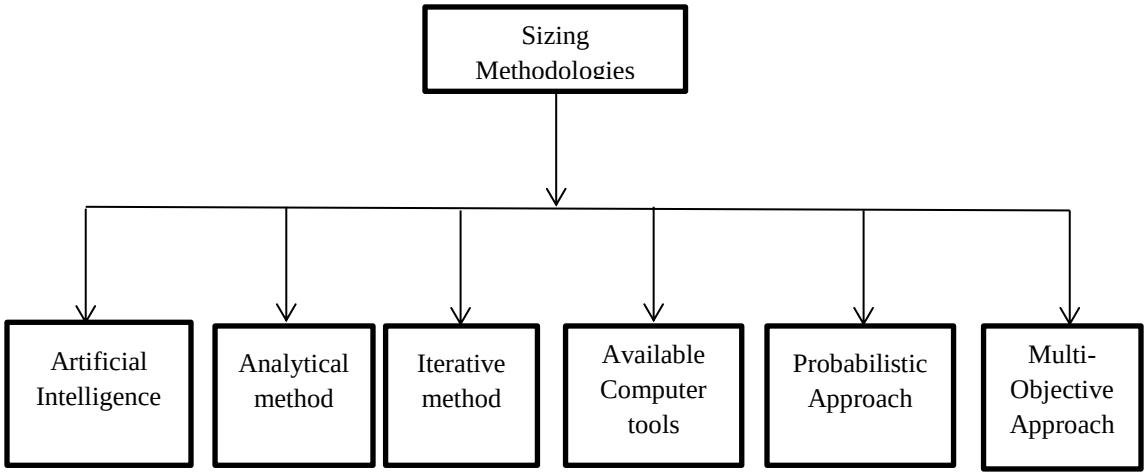

Figure 2.3 Sizing methodologies of IRES [29]

2.1 ITERATIVE APPROACH

Sizing IRES with an iterative method approach is achieved by using typical metrological year (TMY) data such as solar irradiance, wind speed, and temperature. Then, an algorithm is used to find the best economic result using net present value (NPV) and/or levelized cost of energy (LCE) at the required Loss of Power Supply Probability (LPSP), deficiency of power supply (DPSP), or other reliability criteria such as availability of power supply.

Daif et al. [30] used an iterative methodology to apply a technical and economic assessment to optimally size the PV and wind to an isolated microgrid system. The authors used one year of metrological data at three locations in Corsica Island, France. The flow chart in Figure 2.4 provides hourly data of solar irradiance, temperature, and load. These data were applied to PV and wind turbine models to determine how much they much energy is generated to supply the load or charges the battery if there is excess energy. A set of system configurations were generated based upon the required LPSP. After that, an economic analysis was performed to determine the lowest LCE among all system configurations and find the optimal solution. Based on the analysis, the battery bank was chosen to be replaced every 4 years and a daily load of 3 kWh for each residential house was used.

Another study by Parsad and Natarajan [31] showed how iterative optimizing methodology for PV-Wind hybrid system was applied. Software has been developed to provide simulations using various parameters such as deficiency of power supply (DPSP), relative excess power generated (REPG), utilized energy probability (UEP), and LCE of power generation with battery bank. The software allows the designer to select

any location for the hybrid MG system and find the optimal size based upon specified DPSP with minimum life cycle unit cost (LUC). For determining the optimal size, three loops were used. The outer loop is first initiated by sizing the wind machines from various wind machine models. The middle loop is then used to calculate the number of solar panels with each the values assigned to each wind machine model. Finally, the inner loop is used to calculate the energy of the battery storage.

In other research conducted by Yang et al. [32], a Hybrid-Solar-Wind System Optimization Sizing (HSWSO) model was developed to optimize the size of PV and wind power generation capacity using battery energy storage. The model developed in this research includes three parts: the models for PV, wind and battery energy storage, the model for the LPSP, and the model for the LCE. The orientation of the PV module and tower height of the wind turbines are considered part of the sizing methodology which is obtained using long-term weather data and load demand input. The optimal configuration for the hybrid system is obtained using the LPSP and the lowest LCE. The desired LPSP is obtained annually by performing calculations using the number of PV modules, orientation of the PV modules, the rated power of the wind turbine, tower hub height, and capacity of the battery bank. After determining the LPSP, the configuration that has the lowest LCE is chosen. A flow chart illustrating this process is shown in Figure 2.5.

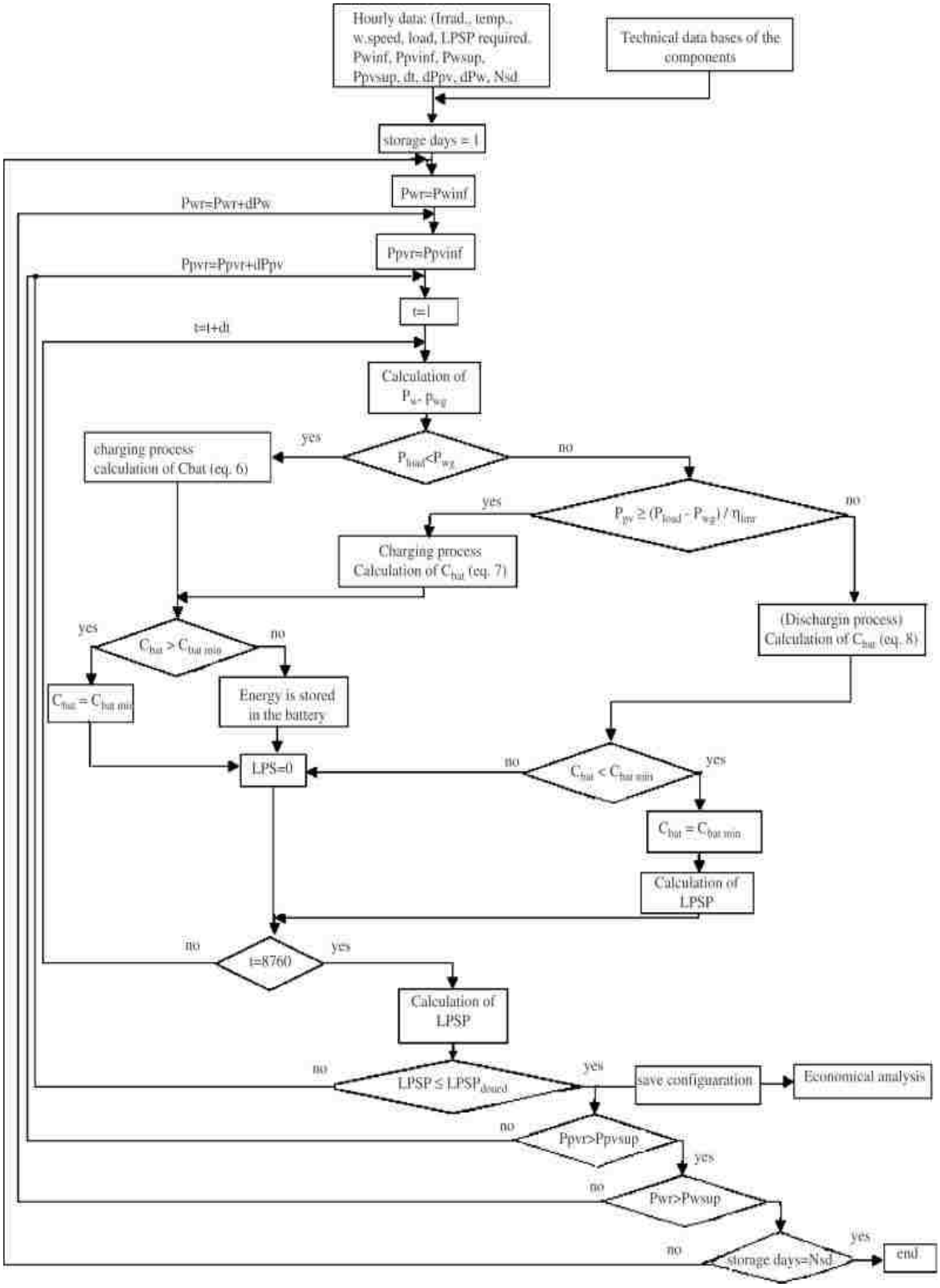

Figure 2.4 Algorithm for optimal sizing of the hybrid PV/ Wind sources [32]

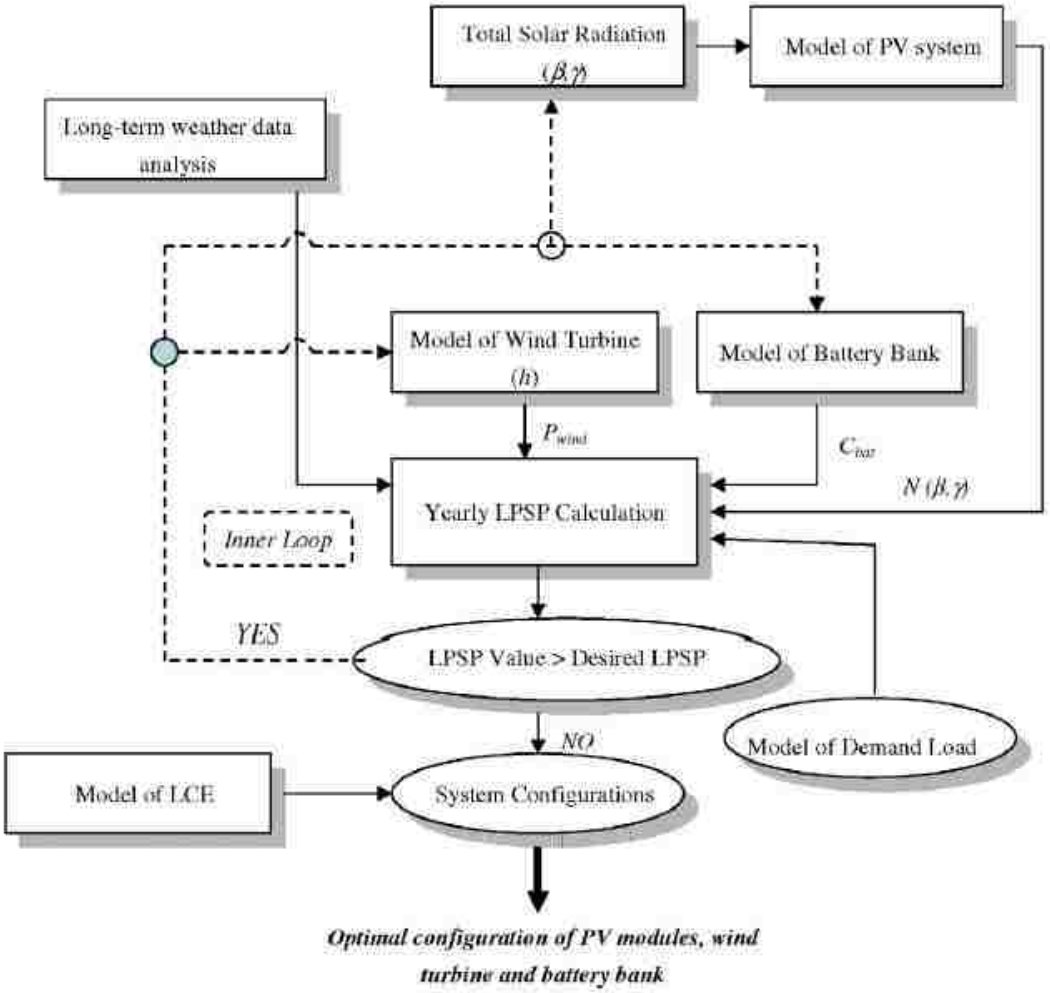

Figure 2.5 Flow chart of the HSWSO method [30].

2.2 ARTIFICIAL INTELLIGENCE (AI) APPROACH

When AI is used, weather data may not be needed to find the proper size for renewable energy resources and battery energy storage. In the literature, numerous AI techniques have been used.

Yang et al. [33] developed a genetic algorithm (GA) to optimally size the hybrid solar-wind system to achieve a LPSP with minimum ACS to meet consumer demands.

When compared to conventional methods, this system yields the global optimum for the hybrid energy system with computational simplicity. The optimization process includes the PV module number, PV module slope angle, wind turbine number, turbine height, and the number of battery units. The researchers applied this method to a telecommunication station in China and found that 3 to 5 days of energy storage with 80% DOD yielded a 1% to 2% of LPSP, respectively. In their study, losses due to system components were not taken into consideration. Thus, the LPSP will be worse than the desired value, a factor which can cause a designer to oversize the system components.

Likewise, Xu et al. [34] used GA to minimize the total capital cost using the constraint of LPSP. The method was applied to a standalone wind/PV MG system. The sizing methodology uses the type and size of WG, tilt angle and size of the PV panels, and the capacity of the batteries. In their proposed methodology, TMY data, including extraterrestrial horizontal radiation, global horizontal radiation, diffuse horizontal radiation, temperature, and wind speed were utilized. The WG ratings used in this study were 1 kW, 3 kW, 5 kW, 7.5 kW, and 10 kW. Each PV panel used had a power rating of $50W_{peak}$. In addition, the battery capacity for each battery was 200 Ah. The round-trip efficiency of the battery bank was 0.7 with 50% DOD and a constant load of 2KW with a 1% LPSP was used.

Askarzadeh developed a novel methodology by merging the following three algorithms: chaotic search (CS), harmony search (HS), and simulated annealing (SA). These three algorithms were combined to find the optimal size of PV panels along with the number of wind turbine and batteries with minimum total annual cost [35]. The constraints for the system were the maximum and minimum number of wind turbines, PV

panels, and number of batteries. Also, the maximum DOD of the battery energy storage was considered as a constraint in this method. Askarzadeh found that the invented discrete chaotic harmony search-based simulating annealing algorithm (DCHSSA) provided a good optimum sizing of the wind/PV hybrid system.

Kumar et al. [36] used a biogeography based optimization (BBO) algorithm to attain global optimum solution to identify the size, control, and power management strategy for the wind/PV hybrid energy system based upon the total cost and ability to insure the availability of power supply. The BBO method leads to an excellent convergence property with less computational time compared to conventional methods.

In contrast to the BBO method, Ekren et al. [37] used a response surface methodology (RSM). This methodology is a collection of statistical mathematical methods used to optimally size PV/wind integrated hybrid energy system with battery storage. Historical hourly mean solar radiation and wind speed data for the past two years were used to develop a simulation model. The simulation model was then used to predict solar radiation, wind speed, and electricity consumption of the load. Following these predictions, a regression metamodel of the hybrid energy system was obtained using the simulation model data. Finally, the RSM optimization technique was used to optimize the metamodel to find the PV area, wind turbine rotor swept area, and battery capacity.

Arabali et al. [38] applied GA based optimization approach with fuzzy C-Means (FCM) to minimize the cost function that guarantees minimum PV, wind generation installation, and storage requirements to supply a controllable HVAC load. Different percentages of load shifting have been used under different scenarios to examine the efficiency of the system. To match the energy generation from PV and WGs with

controllable HVAC load, a smart grid strategy was been applied. By increasing the load shifting percentage, the system becomes more flexible. Also, the efficiency of the system will increase and the excess energy production from renewable resources will decrease. This study shows that the cost of the system increases as the risk of failure increases.

Kashefi et al. [39] also applied an advance variation of particle swarm optimization (PSO) algorithm to optimally design hydrogen-based stand-alone wind/PV generating system. The researchers proposed a reliability evaluation method for the hybrid system to reduce the time and computations. Their main goal in designing a hybrid system was to provide a reliable supply of power to the load under varying weather conditions with minimum system cost. The wind/PV/FC hybrid generating system is designed to operate for 20 years. The novel variation of PSO achieves a global optimum. A MATLAB code was been developed to consider the outage probability of the three major components of the hybrid system, namely the wind turbine generator, PV array, and DC/AC converter. The study then provided a reliability/cost assessment. In addition, factors such as the uncertainty in wind speed, solar radiation, and load data was been considered. The research showed that a DC/AC converter plays a significant role in the reliability of the system and can be considered an upper limit for the system's reliability.

2.3 MULTI-OBJECTIVE DESIGN APPROACH

Optimal sizing of hybrid MG resources a variety of objectives including reliability, cost, and occasionally greenhouse gas emissions. In addition, these objectives might conflict with one another such as reliability and cost. As a result, the problem of optimal sizing of MG energy sources is considered a multi-objective problem (MOP). As

with any problem, there are usually a set of constraints that must be followed to finding a solution. However, an MOP often does not lead to a single solution, but rather provides a set of solutions which are trade-offs between various objectives. Figure 19 shows the trade-offs of the MOP which are the Pareto optimum sets [29].

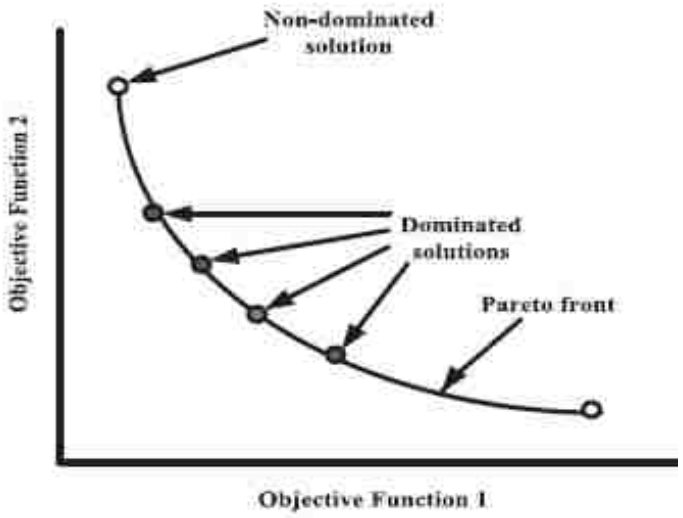

Figure 2.6 Pareto front for a MOP [28]

Katsigiannis et al. [40] applied an evolutionary multi-objective algorithm approach with a non-dominated genetic algorithm (NDGA-II) to solve the MOP of an isolated hybrid MG system. The constraints of the MOP were initial cost, unmet load, capacity storage, fuel consumption, minimum renewable fraction, and component size constraints. The researchers examined this method on the hybrid MG system with two types of energy storage: lead acid batteries and hydrogen storage combined with a fuel cell. They concluded that lead acid batteries were superior to hydrogen storage when

evaluated using economic and environmental criteria. The researchers also used diesel and biodiesel generators in addition to wind and PV energy sources. The use of diesel and biodiesel generators reduced the cost, but increased the greenhouse gas emissions. As a result, the choice of the size of the system's energy sources depends on the designer target of cost and desired environmental effect.

Pedro and Almeida [41] proposed a novel multi-objective method to optimize the size of wind, solar, and hydropower renewable systems. In this method, large-scale demand-side management (DSM) and demand response (DR) technologies were considered. The method used to maximize the renewable energy contribution to peak load while minimizing the intermittence of these sources at minimal cost.

Ould Bilal et al. [42] used a multi-objective genetic algorithm to optimally size a hybrid solar-wind-battery isolated MG system to achieve minimum ACS with corresponding LPSP. The isolated system is located at Potou on the northern coast of Senegal. Three load profiles with the same daily energy demand were proposed to study the effect of load on the system component size. The study concluded that load profile influenced the design criteria which included the cost and system reliability.

Another study by Abbes et al. [43] used a triple multi-objective optimization to combine the LCC, embodied energy (EE), and LPSP. The optimal configuration between the hybrid wind, PV, and battery MG system can be found by using the dynamic model and applying a controlled elitist genetic algorithm for the multi-objective optimization (Figure 20). Both economic and environmental factors have been considered in this study which was designed to investigate the consumption of non-renewable primary energy sources to find the environmental impact on the design criteria. The results show that the

hybrid system is greatly undersized when load shedding is tolerated. As a result, the cost of the system and environmental impact are reduced.

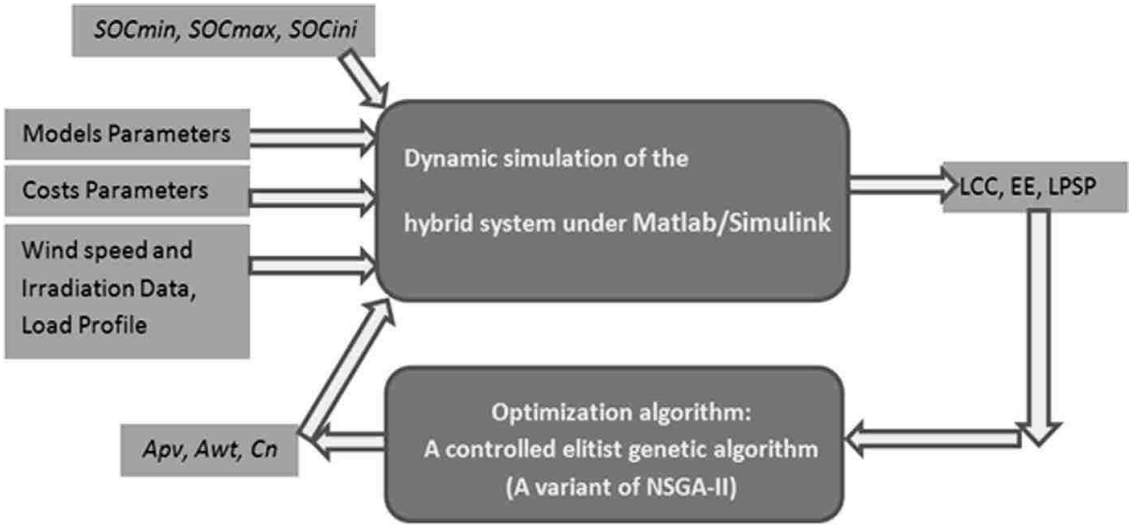

Figure 2.7 Design principal of the MOP [43]

2.4 PROBABILISTIC APPROACH

The probabilistic approach is used to create a risk model from generation and/or load models. Out of all the various optimization techniques, it is considered the simplest method used to optimize the hybrid integrated renewable energy sources. However, it does not yield the best solutions [29]. In the literature, several research papers have been published which use this type of approach.

Karaki et al. [44] developed a general probabilistic approach to optimize an autonomous solar-wind energy system. Various wind turbines and solar modules were

also considered as well as the state of charge (SOC) and how its battery energy storage capabilities satisfy certain load profiles. A model has been developed that represents the modes that the equipment can utilize in the event of failure and the availability of the power supply. Although cost was not considered in this paper, the authors indicated that a production costing program can be associated with their approach.

Yang and Burnett [45] developed a simulation model to analyze the probability of power supply failure for a hybrid wind/PV generation system with battery energy storage. Their model can also be used to analyze the reliability of the system. The simulation showed that solar power and wind power complement each other very well. To study its usefulness, this methodology was applied to a case study of an isolated hybrid MG system to supply power for a telecommunication system. Different desired LPSPs were used to find the optimal combination between the hybrid system components. The study also showed that load profile impacts the priority sequence of which type of system should be selected. The sequence, from best to worst should be the hybrid PV-wind power generation system, wind power system alone, and PV system alone.

Tina and Gagliano [46] performed a probabilistic analysis of weather data for a hybrid PV-wind MG system using long-term meteorological data from Acrieale, Italy. Their proposed approach was to check if the probability distribution functions (PDFs) of Hollands, Huget, and Weibull were good fits for real PDFs of clearness index. The PDFs of each energy source was then calculated. This methodology required knowledge of the daily maximum irradiance and the 3-hour interval per day of wind speed due to non-linearity in wind turbine power curve.

Tina et al. [47] developed a probabilistic design approach to optimize the hybrid PV-wind MG system. This approach is based on the convolution technique to assess long-term performance of a hybrid PV-wind MG system based on Expected energy not supplied (EENS).

2.5 ANALYTICAL METHOD

The analytical method uses computational models of system energy components to describe component size as a function of system feasibility. Once the model is set, system performance can be evaluated according to certain criteria. Long-term meteorological data are needed to perform this methodology.

Khatod et al. [48] applied a systematic analytical approach to optimally size an isolated PV-wind hybrid MG system. The proposed method associated the uncertainties of solar irradiance, wind speed, power demand, and outages of each generating unit. Also, a production-costing simulation was performed and the results were compared using the Monte Carlo simulation (MCS) method. The results of the proposed analytical method were shown to be accurate, computationally efficient, and required less meteorological data than MCS.

2.6 COMPUTER SOFTWARE DESIGN TOOL

There are various computer software packages that provide proper unit sizing for different power generation units in a hybrid MG system. The Hybrid Optimization Model for Electric Renewables (HOMER) is one of the most widely used software programs [29]. HOMER was developed by the National Renewable Energy Laboratory (NREL) and is capable of modeling the physical behaviors of different system components while considering system life cycle costs. The inputs for the HOMER software are load

demand, resource data, component cost, constraints, system control, and emission data. The output data that HOMER software generates are net present cost, cost of energy, unmet load, excess energy, fuel consumption, and renewable energy fraction. When more accurate results are required, the HYBRID2 program is used [29]. This program combines probabilistic and time series models and can model systems with time steps from 5 minutes to 2 hours. The input data for HYBRID2 are load demand, resource data, power system component data, and financial data. The program's output data are a technical analysis, sizing optimization, and financial evaluation [29]. RETScreen is another software tool that was developed by the Ministry of Natural Resources in Canada. It is able to analyze the technical, financial, energy efficiency, and sensitivity factors of a hybrid renewable energy system and can also provide a risk analysis. However, the program does not account for temperature effect on solar PV system performance [29].

2.7 THE FOREVER POWER METHOD

The Forever Power method, developed by Kimball et al. 2009, can iteratively find the optimal size of PV/Wind/battery energy sources based upon availability of power supply and economic criteria. A year around of hourly solar irradiance, wind speed and temperature are needed to find the optimal solution for a particular load at a particular location. Also, information in the manufacturers' data sheets of the PV module and wind generator is needed to be able to execute the Forever Power method. It can lead to a global optimal solution based on system cost.

3. MODELLING OF PV MODULE, WIND TURBINE, AND BATTERY ENERGY STORAGE

3.1 PHOTOVOLTAIC SYSTEM MODELING

Photovoltaic (PV) panels convert sunlight directly into DC electricity. There are many models in the literature that describe the characteristics of PV modules. A typical IV characteristic of PV array is shown in Figure 3.1. It shows the effect of irradiance on the output current of the array.

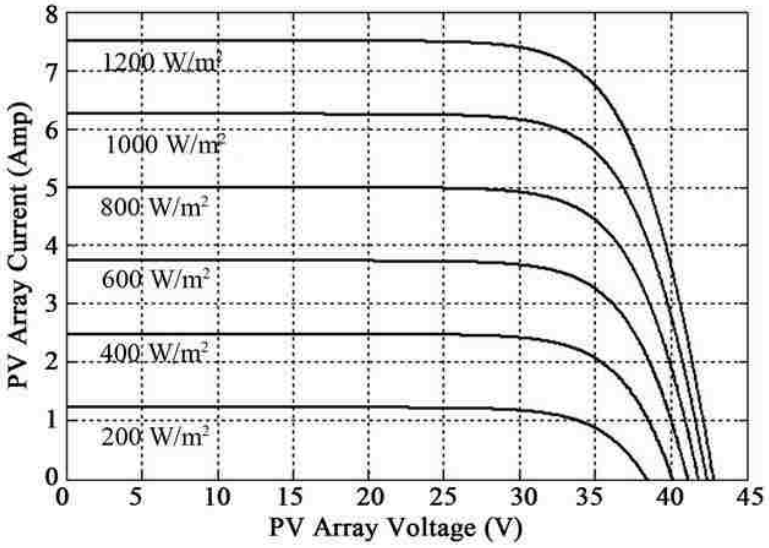

Figure 3.1 Typical IV characteristics of a PV array [49]

The performance of the PV module is highly affected by weather conditions such as solar irradiance and temperature. Figure 3.2 (a) and (b) show how does irradiance and temperature affect the output power and voltage of a typical PV module.

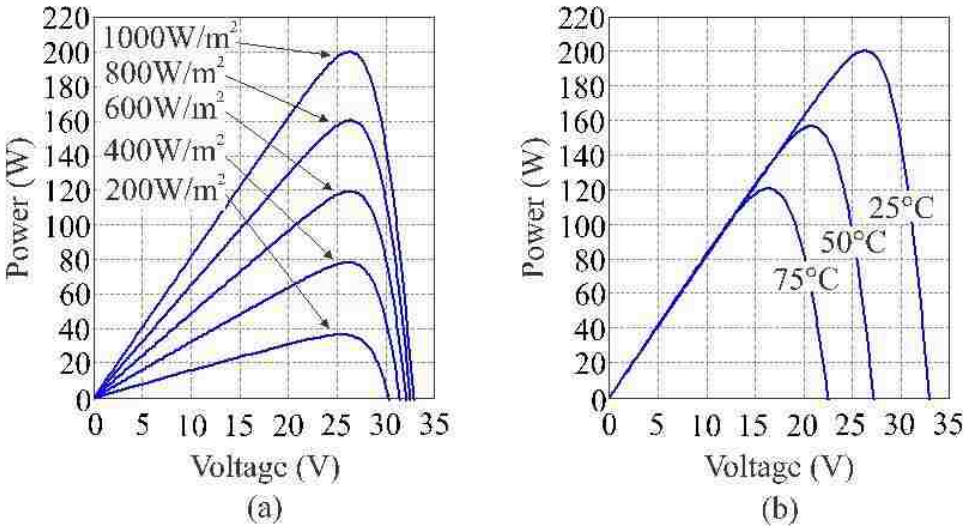

Figure 3.2 Effect of (a) solar irradiance (b) temperature on the output power of a PV module [49]

In this study, a simplified model has been used as follows [43]:

$$P_{pv} = \eta_{pv} A_p G_a \qquad (1)$$

Where, P_{pv} is the output power (W), η_{pv} is the total system efficiency, A_{pv} is the total effective area of the PV panel (m), and G_a is the solar irradiance (W/m^2).

The PV module efficiency is affected by the cell temperature which can be expressed in the following equation:

$$\eta_{pv} = \eta_r \eta_{pc}[1 - \mu\ (\theta c - 25)] \qquad (2)$$

In this equation, η_r is the rated PV module efficiency, η_{pc} is the power converter efficiency, μ is the temperature coefficient at maximum power (/C^o), and θc is the cell temperature (C^o). Also, the cell temperature can be calculated using equation (3) below:

$$\theta c = T_a + \left[\frac{(NOCT-20)}{800} \times G_a\right] \qquad (3)$$

In this equation, T_a is the ambient temperature and NOCT is the normal operating cell temperature. The hourly data of the solar irradiance and temperature can be used to find the hourly output power from each panel once the efficiency of the solar panel and the power converter used are determined and taken into account [43].

3.2 WIND TURBINE MODEL

It is important to choose the appropriate model to determine the performance of a single wind turbine which is characterized by its power curve. The electrical output power of any wind turbine is a function of wind speed and its hub-height. For unit sizing of MG energy sources, many researchers use a simple model that represents the output power curve for any typical WG as shown in Figure 3.3 [51].

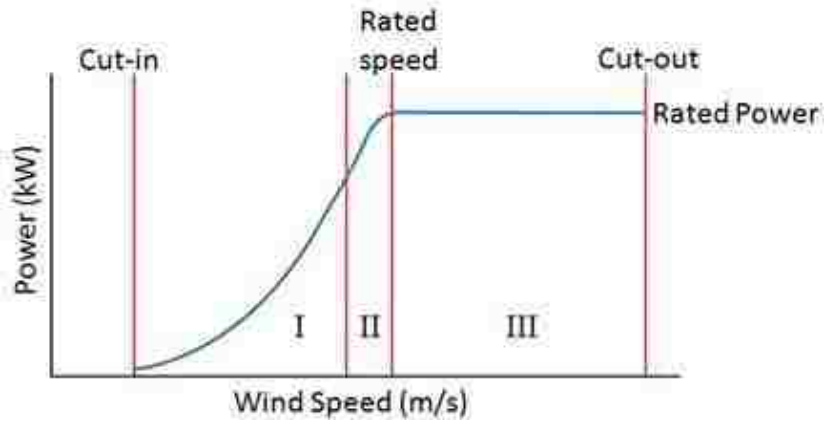

Figure 3.3 WG output power curve [51]

The operating limits of any wind turbine are determined by its cut-in and cut-out speed. Rated power is generated by the WG at the rated speed. These data are provided by the manufacturer of the wind turbine. The following wind power generation output equation is used in most papers [52] [43]:

$$P_w = \begin{cases} P_r \left(\frac{V(t)^2 - V_c^2}{{V_r}^2 - {V_c}^2}\right) & V_c \le V(t) < V_r \\ P_r & V_r \le V(t) < V_f \\ 0 & V(t) < Vc \ or \ V(t) > V_f \end{cases} \quad (4)$$

In this equation, P_w is the output power of the WG, P_r is the rated power of the wind generator, V_c is the cut-in speed of the wind turbine at which the wind turbine begins rotating, V_r is the rated speed of the wind turbine, and V_f is the cut-out speed at which the wind turbine stops rotating. Equation (4) shows that wind speed is squared because it produces power as indicated in manufacturer data sheet. Figure 24 below shows a power curve vs wind speed of a 2.5 kW wind generator which has 2.7 m/s cut-in speed, 25 m/s cut-out speed, and 11 m/s rated speed.

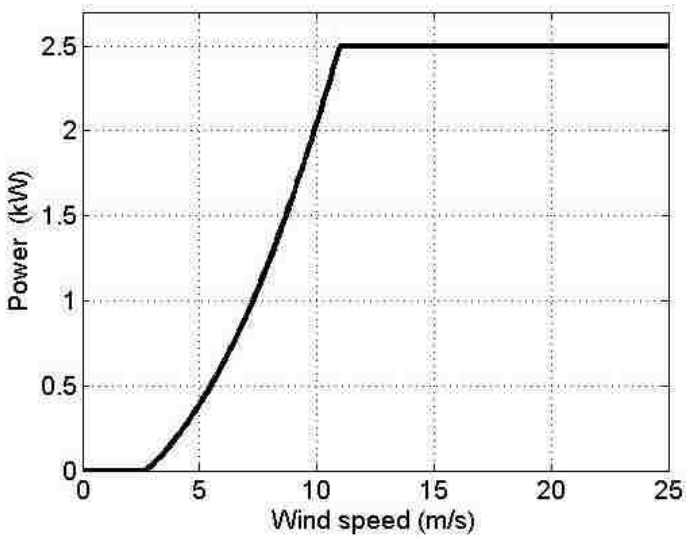

Figure 3.4 Power curve for 2.5 kW wind generator

If the meteorological data recorded were found at a height that was different from the wind turbine's height, the following equation is used to find the new wind speed [43]:

$$V_h = V_{ref}\left(\frac{H}{H_{ref}}\right)^{\alpha} \qquad (5)$$

In this equation, V_h is the wind speed at turbine height (H), V_{ref} is the wind speed recorded by metrological station at height (H_{ref}), and α is the surface roughness factor which is approximately 0.1428 in an open space surface [43].

3.3 BATTERY BANK MODEL

In islanded MG, an energy storage device must be used to balance energy supply and demand. Energy storage devices are used to store energy from renewable sources exceeds the load demand. In times of insufficient energy generation from renewable sources, the energy contained in energy storage devices can be used to supply energy to

the load. Many storage technologies of this kind are available in the market. Each technology has its own characteristics in terms of specific energy (Wh/kg), specific power (W/kg), maturity, siting ease, footprint, and overall cycle efficiency [52]. Electrochemical Battery energy storage (BES) technologies namely Lead Acid (LA), Nickle-Cadmium (NiCd), Nickle-metal hydride (Ni-MH), Lithium ion (Li-ion), and Sodium-Sulfur (NaS) batteries are widely used in MG energy systems [53]. The selection of the appropriate storage technology depends on factors such as reliability and the total cost including life cycle cost, round trip efficiency, low self-discharge, time response, high discharged rate, and high recharge rate [54]. Table 3.1 provides a comparison of rechargeable electrochemical batteries in terms of capital cost while Table 3 provides information about the technical differences of the batteries [54] [55]. Another type of storage batteries is the flow type such as Vanadium Redox Battery (VRB) [54]. It is a mature type of flow battery system where energy is stored using vanadium redox couples (V^{2+} /V^{3+} and V^{4+} /V^{5+}) in two electrolyte tanks [55]. VRBs can operate for more than 10,000 cycles [55]. Also, they have quick responses and relatively high efficiencies of up to ~85%, other characteristics are shown in table 3.2.

Table 3.1 Capital cost of battery energy storage

System	Capital cost	O&M cost
	$ /kW	$/kW-year
LA	300–600	50
NiCd	500–1500	20
Li-ion	1200–4000	_
NaS	1000–3000	80
VRB	600–1500	70

Table 3.2 Comparison of properties of different types of battery storage technologies

Technology	Power rating (MW)	Discharge time	Discharge losses (day)	Suitable storage duration	Cycling capacity	Life time (years)
NaS	0.05–8	Seconds–hours	~20%	Seconds–hours	2500	10–15
Ni–Cd	0–40	Seconds–hours	0.2–0.6%	Minutes–days	2000–2500	10–20
Lead–acid	0–20	Seconds–hours	0.1–0.3%	Minutes–days	500–2000	5–15
Li-ion	0–0.1	Minutes–hours	0.1–0.3%	Minutes–days	1000–10,000+	5–15
VRB	~ 0.03–3	Seconds–hours	Small	Hours–Months	+10,000	5-10

Lead acid batteries are one of the most widely used energy storage technologies in an MG system because they have low energy cost per kWh ($300-$600 per kWh) and it is a mature technology [55]. Lead acid batteries have low self-discharged rates of less than 0.3% and a high cycle efficiency of up to 90% [55]. Deep cycle lead acid batteries are designed to withstand more deep discharge cycles which make them a good choice for an islanded MG system. There are two types of deep cycle lead acid batteries, flooded and valve-regulated. The valve-regulated type includes Absorbent Glass Mat (AGM) and gel technologies to eliminate the need for water addition. Battery life cycle is affected significantly by the DOD, current, performance of charge controller, temperature, and duration of time the battery at a low SOC [56] [57]. Temperature effects on the capacity of lead acid batteries and their lifespan are often ignored because of the assumption that the battery bank is in a climate control system [58]. In this research, only DOD is considered from the manufacturer data sheet. Figure 3.5 shows a typical curve that represents the number of cycles versus the DOD of the battery [56]. There are many

models used to predict the lifetime of LA batteries in stand-alone applications. Dufo-Lopez et al. compared different LA battery lifetime prediction models for stand-alone PV systems [59]. In his paper, the estimation of battery life cycle in many research simulations for optimal sizing of micro-sources in an isolated MG systems were found to be substantially lower than the actual cycles [59]. For example, HOMER software overlays estimate the life cycle of the battery bank to be 9 years with greater than 50% DOD cycling and 15 years at 20% DOD [57]. The battery cycle lifetime provided in data sheets are obtained using standard test conditions which are often lower than the conditions used to cycle MG in MG stand-alone applications [59].

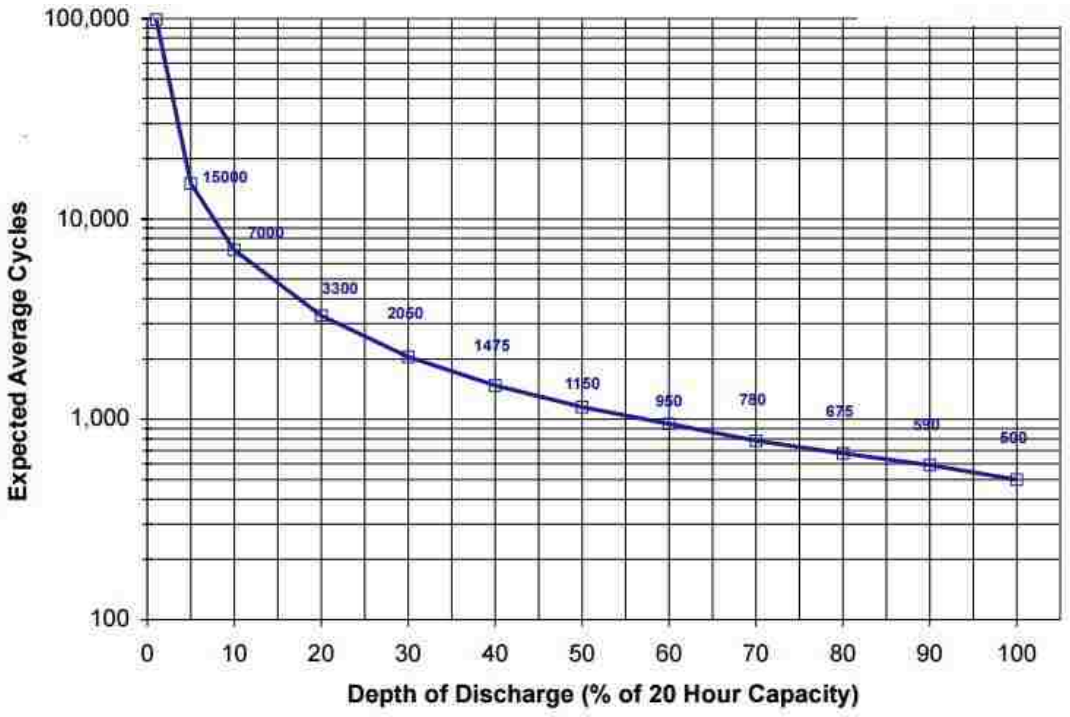

Figure 3.5 Effect of DOD on the battery life cycle [57]

To represent the SOC of the battery storage, the following simplified model is used [43] [31]:

$$\text{SOC (t)} = E_B(t-1) + [E_g(t) - E_L(t)]\eta_B \qquad (6)$$

$$DOD(t) = 1 - SOC(t) \qquad (7)$$

In this equation, t represents the time in hours, E_B is the remaining battery energy capacity, E_g is the generated power by the PV modules, WG, E_L is the load energy demand, and η_B is the round trip efficiency of the battery storage.

In a hybrid MG system, it is important to measure the excess power generated (EPG) to find the annual excess amount of power generated by the hybrid micro-sources [30]. For any combination of PV/Wind/battery system, there will be times when load demand is lower than the load generation and the excess power is not utilized due to fully charged battery energy storage. EPG is defined as ratio of the total annual excess of power generated by the hybrid micro-sources in a MG system in year to the total annual load in the year. The following equation represents this relationship [30]:

$$EPG = \sum_{t=1}^{h}[E_B + (E_g - E_L)] \qquad (8)$$

The remaining utilized energy (UE) is used for the economic evaluation of system cost and can be found using the following equation:

$$UE = (EG - EPG) \qquad (9)$$

In this equation, EG is the energy generated by the PV modules and WGs.

4. THE FOREVER POWER METHODOLOGY FOR THE OPTIMAL SIZING PROBLEM

4.1 INTRODUCTION

The Forever Power method is an iterative method that uses the number of PV modules, WGs, and the capacity of battery storage units to achieve the targeted availability of power supply, the fraction of the time when energy is available, and economic criteria [59]. This method was first introduced by Kimball et al. to find the optimal size of PV/battery hybrid system [60].

4.1.1 Reliability Criteria. Availability is markedly different from reliability. Reliability is the ability of a system to operate without failure while availability is the fraction of time at which the energy is available to the load throughout the system life cycle. However, a highly reliable renewable energy system does not guarantee high availability of power due to insufficient energy storage. Therefore, assuming that a hybrid energy system is reliable, the availability of power supply can be used as a criterion of reliability. The Forever Power method in Figure 26 has been used to provide hourly checks that the power demand by the load (P_L) is met while the energy content of the battery bank does not fall below the minimum DOD. In this flowchart, *n* and *m* are the number of PV modules and WGs, respectively, Ppv is the power generated by PV modules, and Pw is the power generated by WGs. To find all availabilities and LCOE that correspond to all combinations of PV modules and WGs, the flow chart in Figure 4.1 is used. To apply this method, the hourly data of solar irradiance, temperature, and wind speed of the selected location for the MG. Moreover, other data are taken from

manufacturer technical sheet such A_{pv}, η_r, η_{pc}, NOCT, P_r, V_f, V_r, V_c, and hub height of the wind turbine.

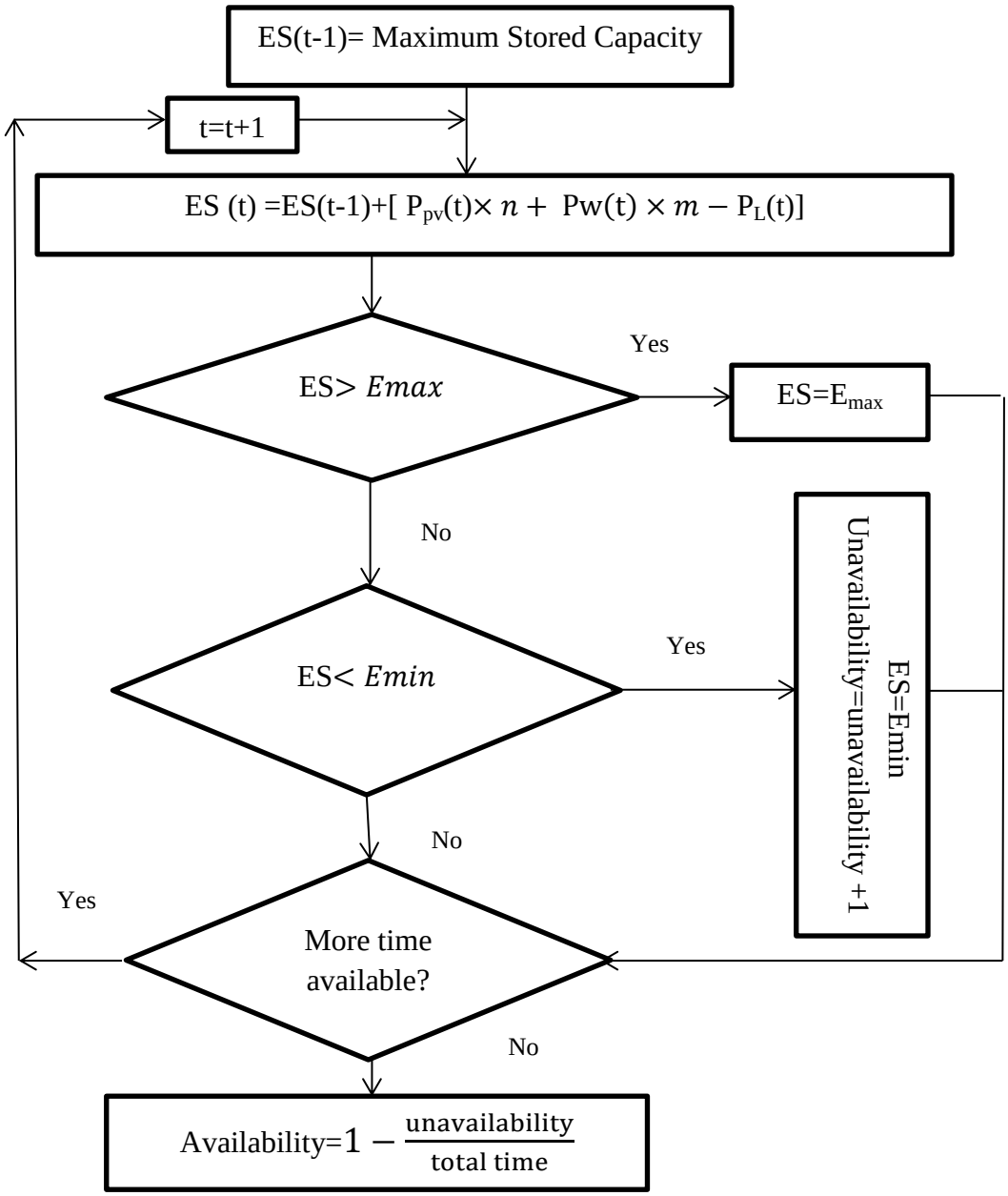

Figure 4.1 The Forever Power loop

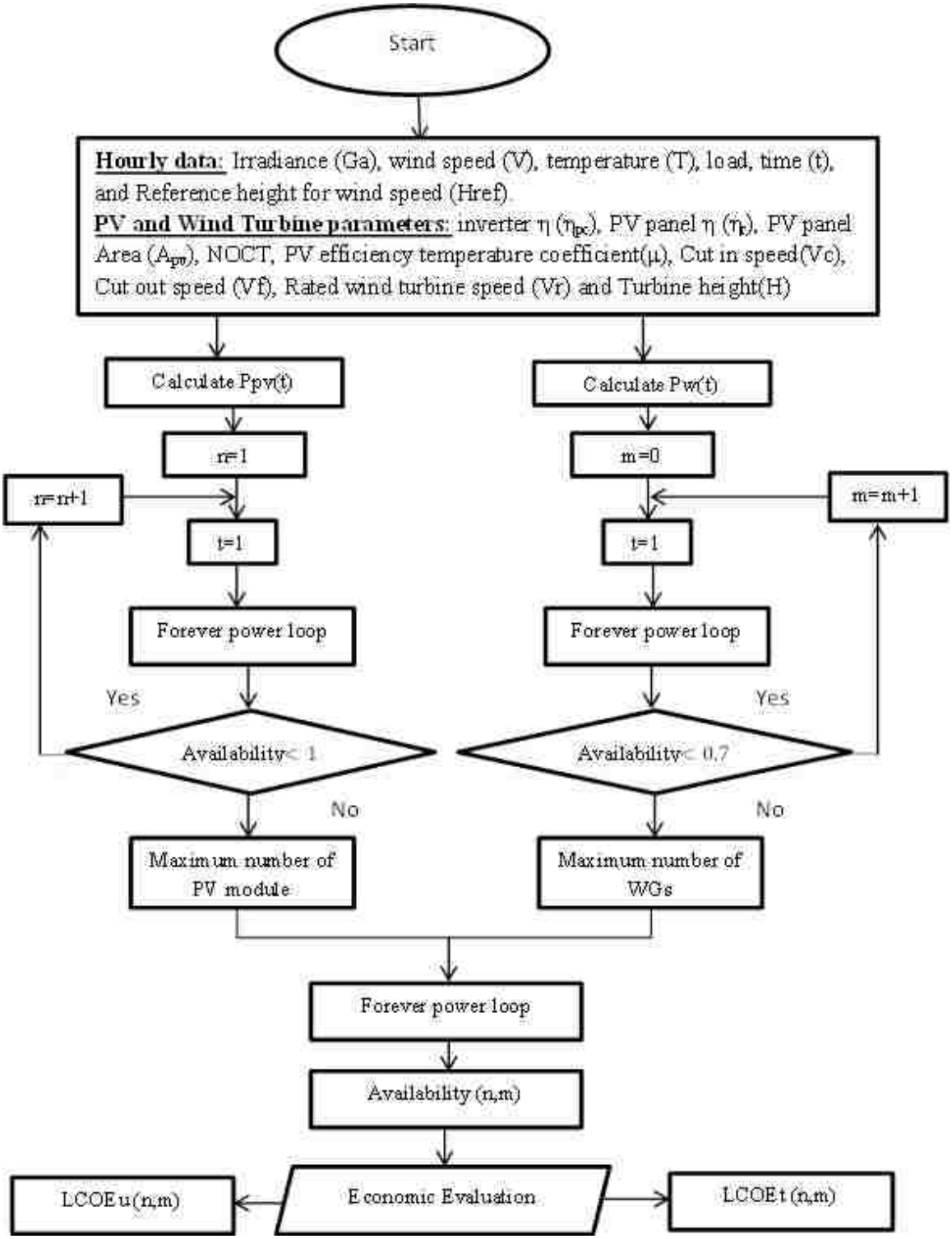

Figure 4.2 Overall Algorithm for unit sizing of PV/Wind/Battery Hybrid MG system

The Forever Power algorithm is applied to the PV module alone with battery energy storage to find the maximum number of PV modules needed to reach 100% availability of power. The algorithm is then applied to the WG alone to determine the maximum number of WGs needed to reach 70 % availability of power. These algorithms are shown in Figure 4.2. Following these calculations, a total power matrix can be created which contains all combinations of PV modules and WGs as shown in (10) below.

$$P_t = \begin{bmatrix} P_{pv} & (P_{pv} + P_w) & \dots & (P_{pv} + mP_w) \\ 2P_{pv} & (2P_{pv} + P_w) & \dots & (2P_{pv} + mP_w) \\ \vdots & \ddots & & \vdots \\ nP_{pv} & \dots & & (nP_{pv} + mP_w) \end{bmatrix} \quad (10)$$

Finally, the total power matrix is used again with the forever power loop of Figure 26 to find the availability matrix below (11).

$$Avail = \begin{bmatrix} avail_{11} & avail_{12} & \dots & avail_{1m} \\ avail_{21} & avail_{22} & \dots & avail_{2m} \\ \vdots & \ddots & & \vdots \\ avail_{n1} & \dots & & avail_{nm} \end{bmatrix} \quad (11)$$

4.1.2 System Cost. The cost of an integrated hybrid PV/wind/battery MG system plays an important role in choosing the optimal size of the system components. To satisfy the economic requirements of the optimal system size, researchers have investigated many economic measures. To determine the optimal size of a system from an economic viewpoint, researchers used methods such as measure the internal rate of return (IRR), payback period, return of investment (ROI), and levelized cost of energy (LCOE). In this study, LCOE was chosen to select the best economic result. It includes the total energy generation from each source and the replacement, maintenance, and operation costs of the system components. LCOE is measured in $/kWh which can be

easily compared to the cost of electricity from the utility. LCOE can be measured according to equation (12) below:

$$LCOE = \frac{LCC}{UE\ in\ kWh} \qquad (12)$$

In this equation, LCC is the life cycle cost of the system components and UE is the utilized energy in kWh. LCC includes initial, replacement, maintenance, and operational costs. The objective of calculating the LCOE is to find the minimum value among all combinations of PV/wind/battery energy sources with the targeted availabilities of power supply. This can be achieved by minimizing the LCC and/or increasing the UE. In this case, the availability of the power supply matrix can be used to determine the minimum value of LCOE. To determine the total LCC of the system components, the LCC of the PV system (LCC_{pv}), LCC of wind generation system (LCC_{w}), and LCC of the battery energy system (LCC_{B}) must be found. The following expressions are used to find the present worth (PW) of capital cost for each system component [43]:

$$\mathrm{PWc} = \mathrm{Pr} \times \mathrm{Co} \qquad (13)$$

$$\mathrm{Pr} = \left(\frac{1+\mathrm{i}}{1+\mathrm{d}}\right)^{\mathrm{n}} = \mathrm{x}^{\mathrm{n}} \qquad (14)$$

In this equation, Co is the component capital cost, Pr is the present worth factor for each component which will be the purchased *n* years later, *i* corresponds to the inflation rate, and *d* represents the discount rate.

As a result, the following expression is used to find the LCC of each system component [43]:

$$\mathrm{LCC} = \mathrm{PWc} + \mathrm{PW}_{\mathrm{maint}} + \mathrm{PW}_{\mathrm{replace}} \qquad (15)$$

In this equation, PW_{maint} is the present worth of maintenance cost of each component and can be calculated using the cumulative compound factor as follows [43]:

$$\mathrm{PW_{maint}} = \mathrm{C_{maint}} \quad (x)^2 \left(\frac{1-x^n}{1-x}\right) \quad (16)$$

In this equation, C_{maint} is the maintenance cost value taken as a percentage of the capital cost. In this study, it is assumed that the present worth of replacement cost is zero for the PV and wind throughout the system life cycle because the replacement of the power converters is included in the maintenance cost. The battery energy storage is assumed to be replaced four times for the project life cycle and is measured as follows (17):

$$\mathrm{PW_{replace,b}} = Co\,.\mathrm{x}^{\mathrm{n}-\frac{n}{5}} + Co\,.\mathrm{x}^{\mathrm{n}-\frac{2n}{5}} + Co\,.\mathrm{x}^{\mathrm{n}-\frac{3n}{5}} + Co\,.\mathrm{x}^{\mathrm{n}-\frac{4n}{5}} \quad (17)$$

The capital cost of a wind turbine [63] is composed of 65% for turbine, tower, and converter. The remaining 35% is composed of the cost of installation, cables, connectors, and protective measures. The maintenance cost is considered to be 2% of the capital investment in the wind energy system.

The cost of a PV system [61] is composed of 50% for the cost of modules and 50% for the cost of installation, converter(s), and racking system. The maintenance cost is considered as 1% of the total capital cost of the PV energy system.

Using equations from 8 to 17, the EPG matrix, UE matrix, and total LCC matrix for all combinations of PV/wind for a particular battery capacity can be determined and used to find the LCOE matrix as shown below (18-21):

$$EPG_{n\times m} = \begin{bmatrix} EPG_{11} & EPG_{12} & \dots & EPG_{1m} \\ EPG_{21} & EPG_{22} & \dots & EPG_{2m} \\ \vdots & \ddots & & \vdots \\ EPG_{n1} & \dots & & EPG_{nm} \end{bmatrix} \quad (18)$$

$$LCC_{n\times m} = \begin{bmatrix} LCC_{11} & LCC_{12} & \dots & LCC_{1m} \\ LCC_{21} & LCC_{22} & \dots & LCC_{2m} \\ \vdots & \ddots & & \vdots \\ LCC_{n1} & \dots & & LCC_{nm} \end{bmatrix} \quad (19)$$

$$UE_{n\times m} = \begin{bmatrix} UE_{11} & UE_{12} & \dots & UE_{1m} \\ UE_{21} & UE_{22} & \dots & UE_{2m} \\ \vdots & \ddots & & \vdots \\ UE_{n1} & \dots & & UE_{nm} \end{bmatrix} \quad (20)$$

$$LCOE_{n\times m} = \begin{bmatrix} LCOE_{11} & LCOE_{12} & \dots & LCOE_{1m} \\ LCOE_{21} & LCOE_{22} & \dots & LCOE_{2m} \\ \vdots & \ddots & & \vdots \\ LCOE_{n1} & \dots & & LCOE_{nm} \end{bmatrix} \quad (21)$$

Finally, prices of kWh for each combination of PV/wind and battery storage capacity can compared. Also, a minimum cost can be determined that corresponds to each value in the availability of power supply.

5. APPLICATION ON A RURAL VILLAGE AT YANBU

5.1 ELECTRICAL LOAD

5.1.1 Variable Load. This study assumes 4 houses with two apartments at each house located at a rural area near Yanbu city in Saudi Arabia. The hourly loads patterns of these houses are assumed to be identical and were taken from Alaidroos and He paper [62]. According to [62], the total load for a residential community at Yanbu was obtained from Marafiq utility company. Then, Alaidroos and He [62] implemented a building energy simulation using eQuest to generate the hourly electrical load for the residential community. The average electrical load for the four houses is 21 kWh. The monthly energy consumption of these houses is shown in figure 5.1.

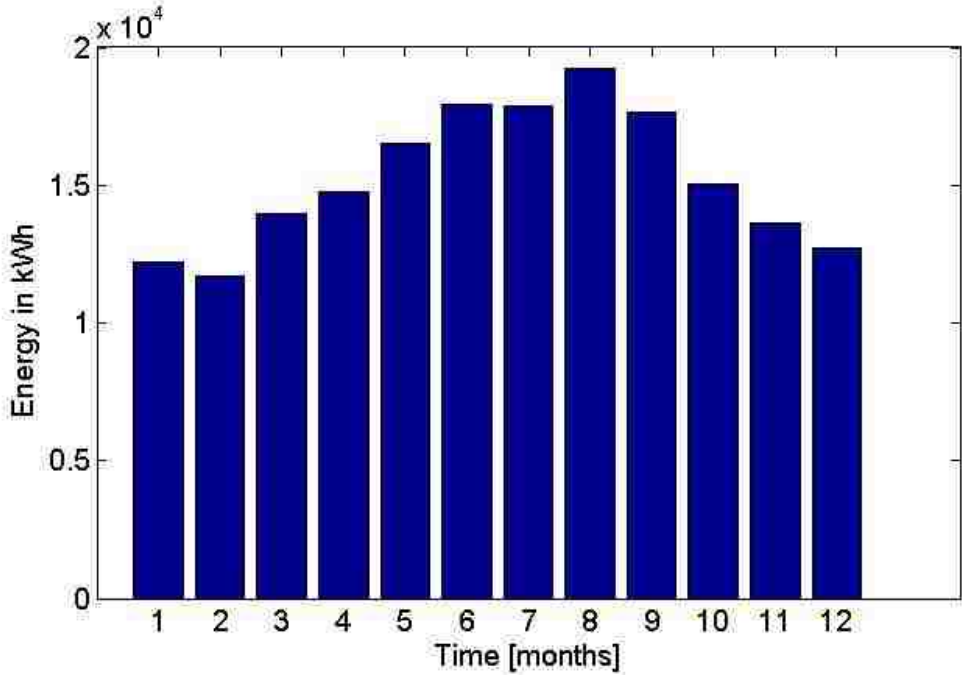

Figure 5.1 Monthly consumptions by the village

Figure 5.2 shows the load variation versus temperature for 1st of January and 1st of August months. As shown, the temperature in the month of August causes the electricity demand to increase due to large air conditioning loads. While, in the month of January the temperature is low and no air conditioning is used.

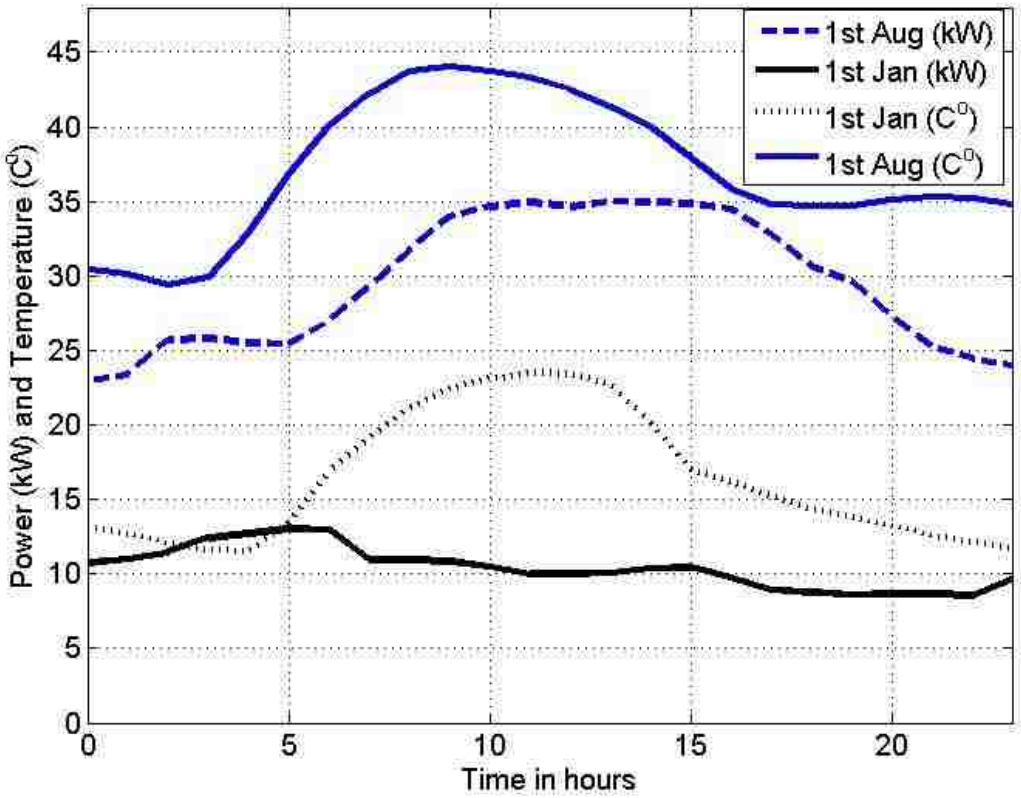

Figure 5.2 Load and temperature variations versus time for one day in January and August

It is shown in figure 5.2 that during summer the energy consumption increases. For example, energy consumption in August is about 50% more than in January due to heavy

air conditioning needed during summer. Figure 5.3 shows the long term minimum and maximum average temperature variation at Yanbu from 2007 till 2014. The maximum temperature recorded at Yanbu during this period is about 48.5^{o}C (119.3 F) and a minimum value of 7.8^{o}C (46.04 F).

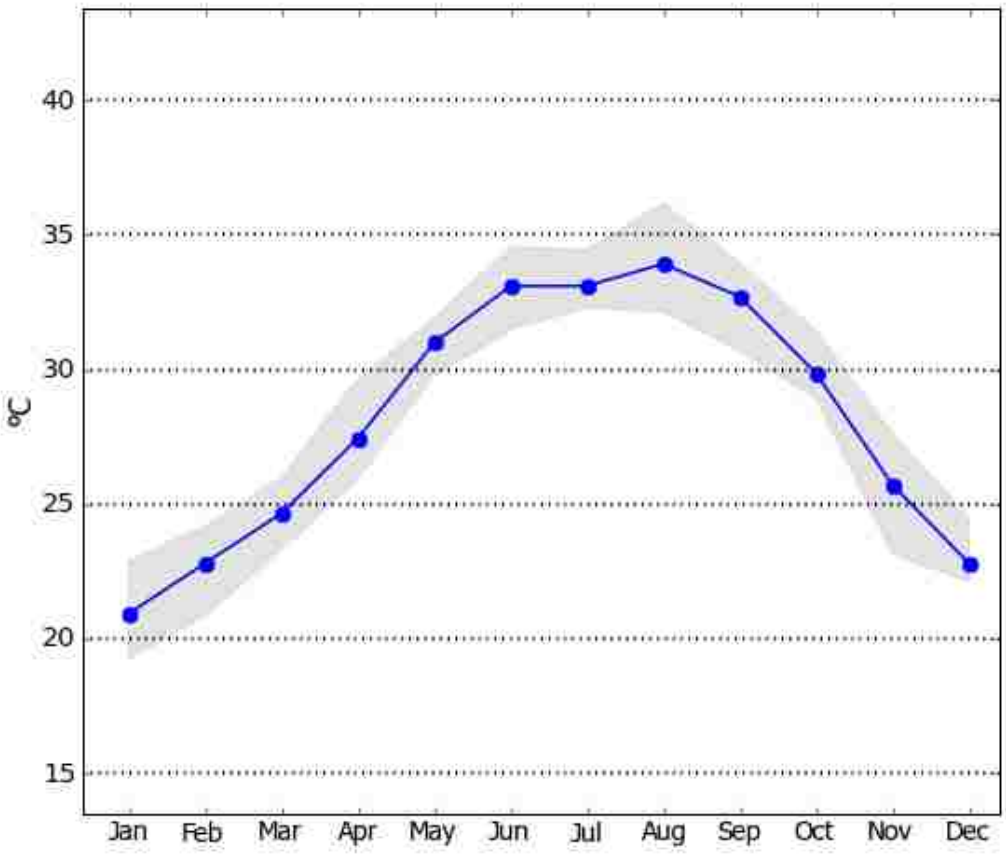

Figure 5.3 Long term average temperature variation at Yanbu (2007-2014)

5.1.2 Applying the Forever Power Iterative Method. To apply the Forever Power iterative method, a fixed value of battery energy storage capacity is used to test the methodology. In literature, it is common to select a three days storage capacity [43]. Since the load is variable, the average energy per day varies from a minimum of 499.2kWh/day in January and a maximum of 775.92kWh/day in August. The average energy per day between these two extremes is 637.56kWh/day. As a result, the three days storage capacity considered in this study is 2000 kWh. Table 5.1 and 5.2 shows the data of the PV module and the WG required for the Forever Power loop.

Table 5.1 PV Module type

Manufacturer	Astronergy
Power at STC	305 W
NOCT	47 C^o
$\boldsymbol{\eta_r}$	15.7%
$\boldsymbol{\mu}$	-0.445%
$\boldsymbol{A_{pv}}$	1.944

Table 5.2 Wind generator type

Manufacturer	Polaris America LCC
Power at rated speed	25 kW
Rated speed	10 m/s
Cut in speed	2.7 m/s
Cut out speed	25 m/s
Tower Height	30 m

The following combinations of PV modules and WGs were obtained as shown in figure 5.4.

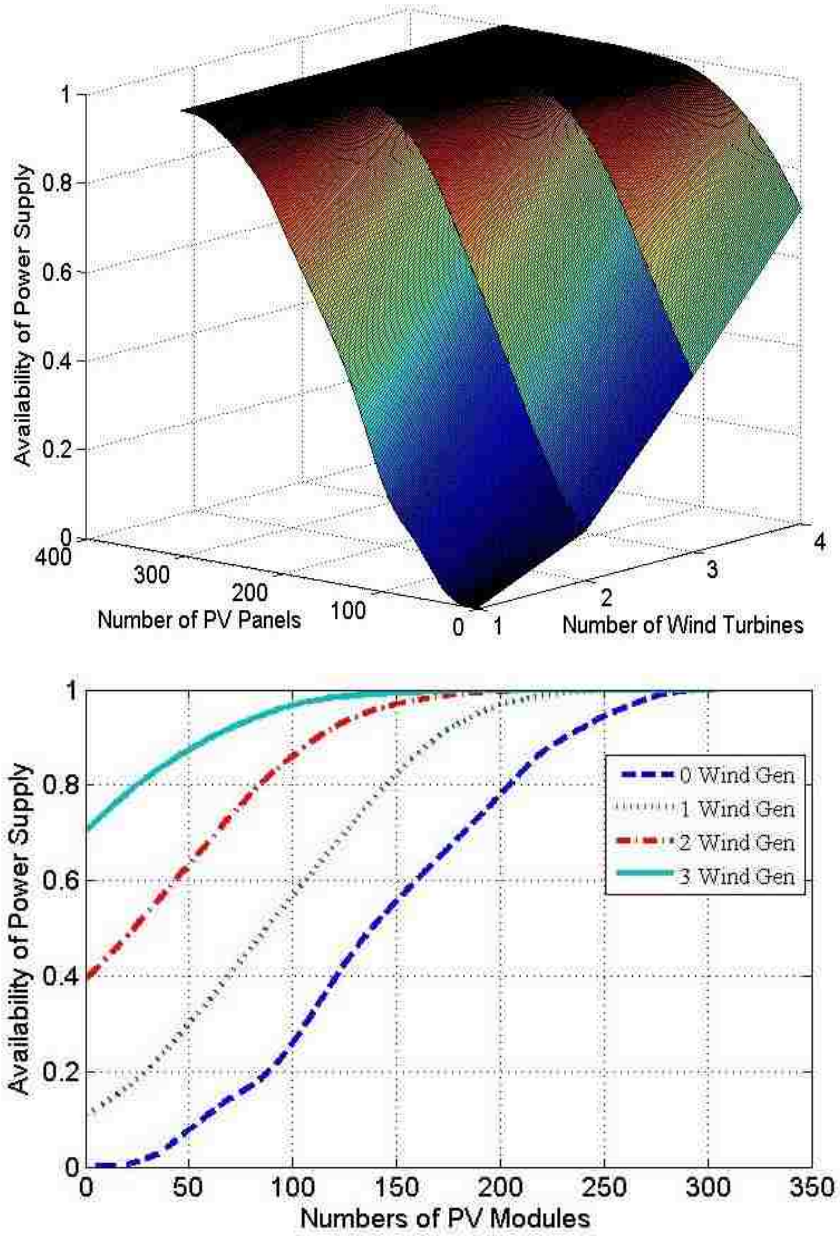

Figure 5.4 Numbers of PV modules and WGs with their corresponding availability for 2000 kWh storage

5.1.3 Calculating the LCOE of the Hybrid MG System. The LCOE is then found by the economic evaluation loop of all combinations of the numbers of PV modules, WGs and battery storage MG system as shown in Figure 5.5. The figure shows the LCOE when all the energy generated is utilized ($LCOE_t$) and when the EPG is not utilized ($LCOE_U$). It is assumed that EPG is utilized at no extra cost. It is shown that the difference between the LCOEt and $LCOE_U$ decreases as the number of WGs increase. For example, in this particular application the $LCOE_U$ decreases by from 0.7833 $/kWh to 0.6622 $/kWh when numbers of WGs used increase from zero to maximum as indicated in table 5.3.

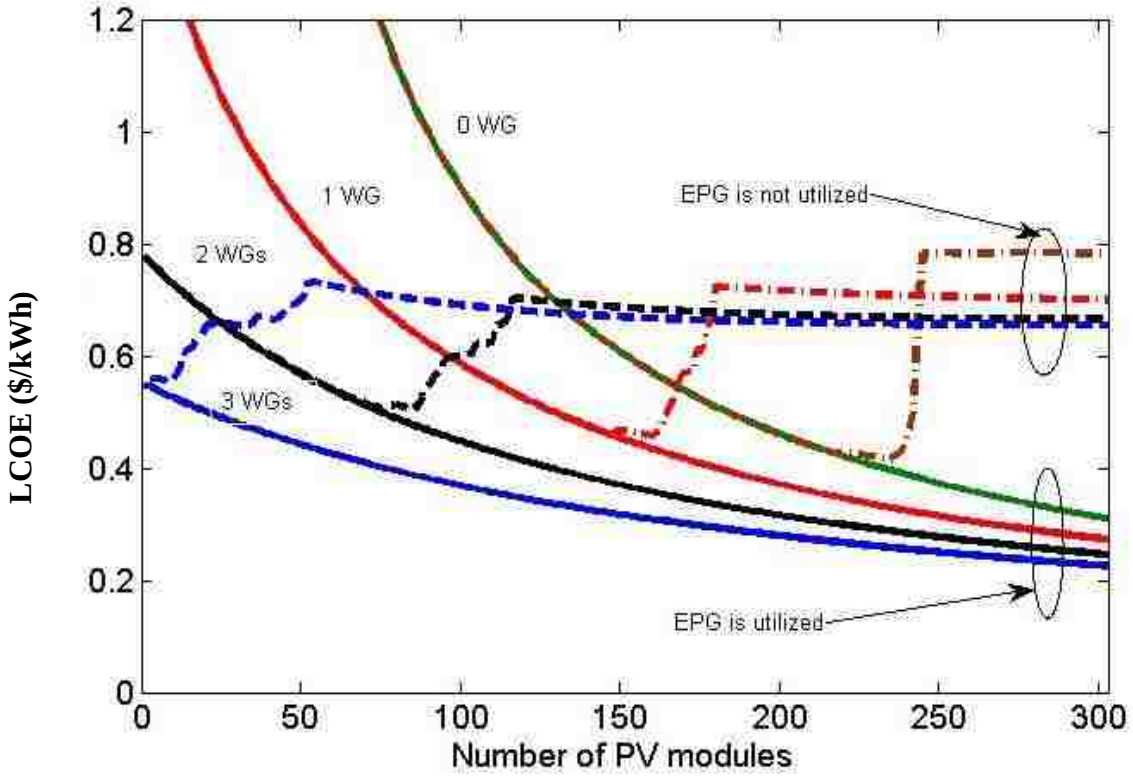

Figure 5.5 LCOE of all numbers of PV/wind energy sources with/without utilizing EPG

Table 5.3 below shows a comparison between two values of availabilities (99.5% and 100%) with their LCOE including and excluding EPG. It is observed that when EPG is utilized the LCOE has the lowest value using maximum number of WGs while it has the highest value when EPG is not utilized. Also, decreasing the availability of power supply by 0.5% led to a decrease in the numbers of PV modules by 18, 21, 28, and 38 modules with 0 to 3 WGs respectively. Consequently, the $LCOE_U$ and LCOEt have the lowest value when three WGs are used. However, the decreasing numbers of PV modules did not lead to a lower LCOE compared to 100% availability. That is because the amount of energy generated by the numbers of PV modules used in the 100% availability is greater in terms of cost than the cost of the number of PV modules saved throughout the system life cycle. On the other hand, the increase of $LCOE_U$ is negligible when there is a decrease of 0.5% in the availability of power supply.

Table 5.3 LCOE corresponding to two values of availabilities of power supply

Storage kWh	**2000**							
Availability	**99.50%**	**100%**	**99.5%**	**100%**	**99.5%**	**100%**	**99.5%**	**100%**
number of PV modules	285	303	231	252	192	220	158	196
number of Wind Generators	0	0	1	1	2	2	3	3
LCOEt ($/kWh)	0.3195	0.311	0.3345	0.3135	0.3242	0.2997	0.3112	0.2826
$LCOE_U$($/kWh)	0.7857	0.7833	0.7108	0.7071	0.6765	0.672	0.6691	0.6622

Then, the SOC of the battery energy storage for each solution is shown in figure 5.6 (a,b), and figure 5.7 (a, b).

(a)

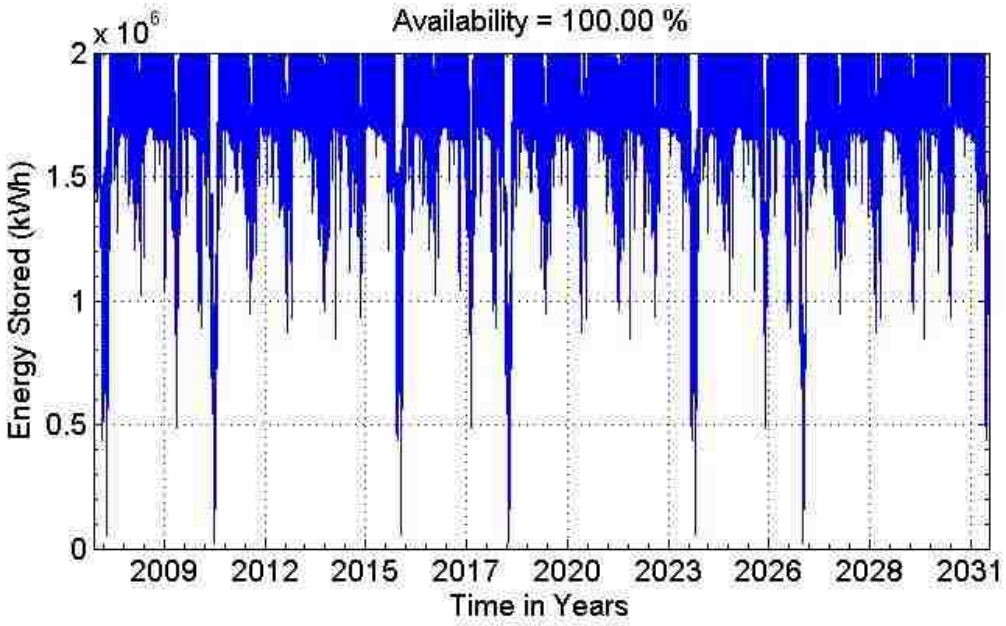

(b)

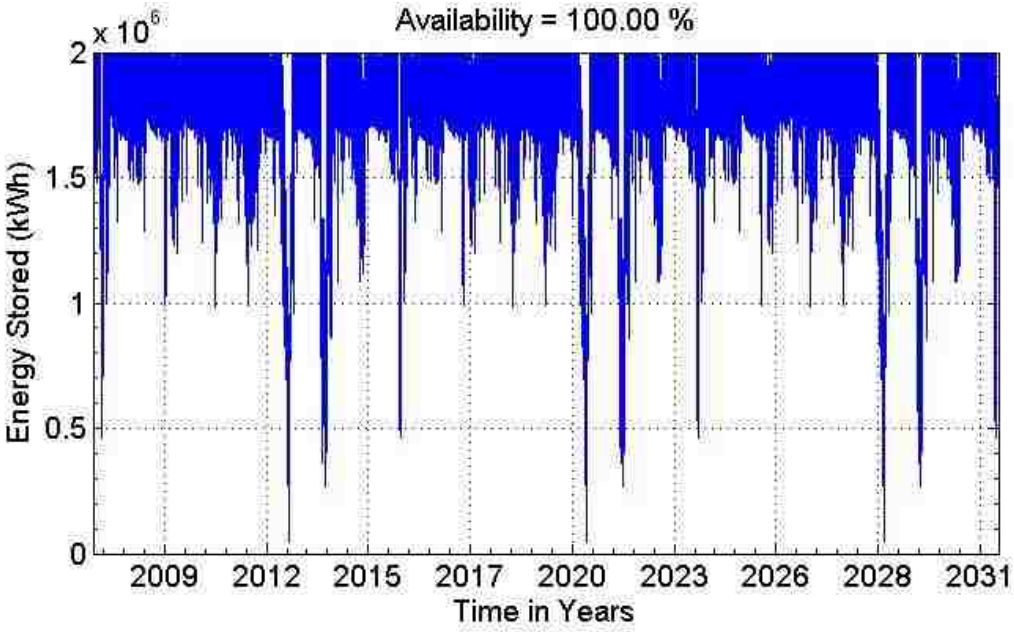

Figure 5.6 SOC of the battery storage throughout the system life cycle (a) Only PV modules (b) PV modules with One WGs

(a)

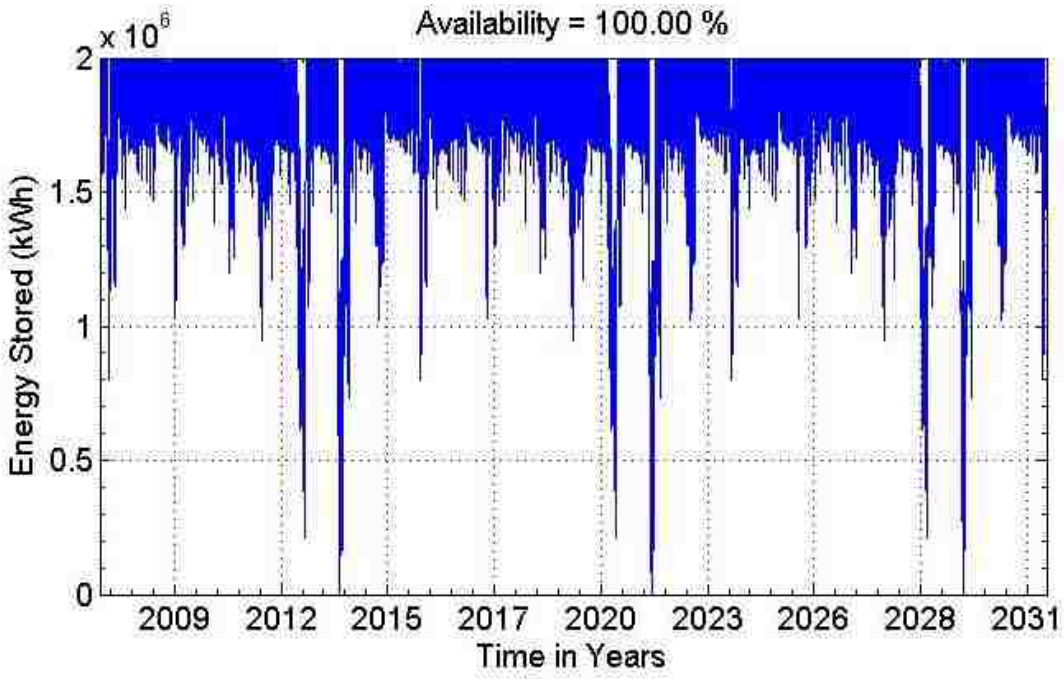

(b)

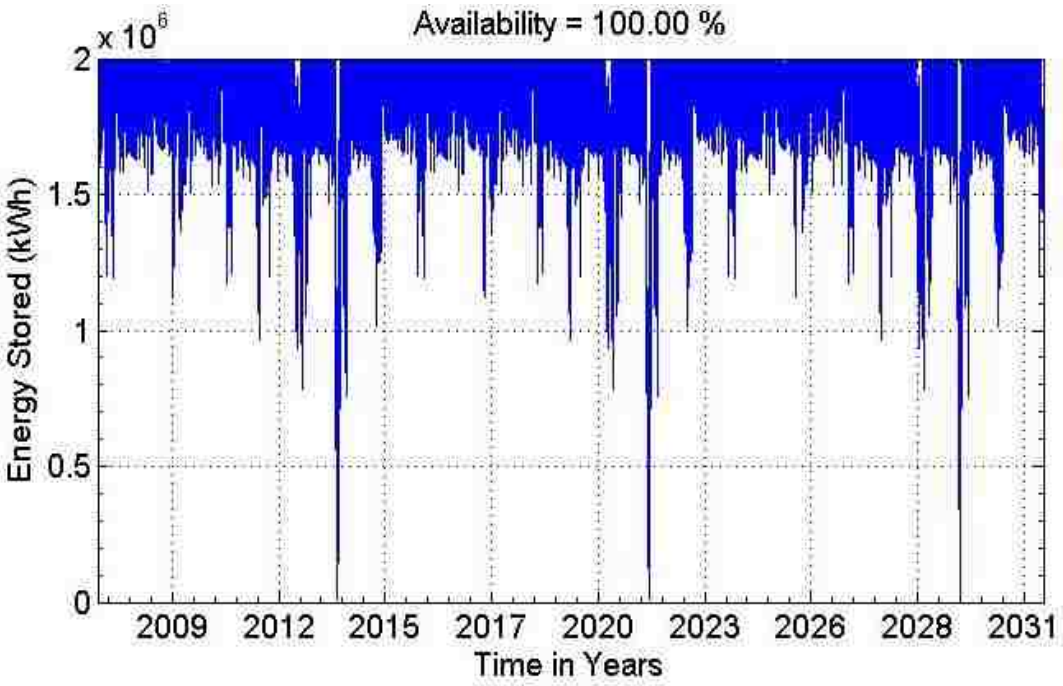

Figure 5.7 SOC of the battery storage throughout the system life cycle (a) PV modules with two WGs (b) PV modules with three WGs

It is hard to tell from figures 5.6 and 5.7 which solution leads to a better performance of battery storage in terms of SOC. Consequently, table 5.4 shows the number of cycles the battery went above 80% and 50%, while the SOC goes below 30% and 10% for all solutions. Table 5.4 shows that as the number of wind generators increases, the cycles at which the SOC of the battery go above 50%. Also, it is shown that the cycles of the SOC of all solutions are more than 95% of the time above the 50%.

Table 5.4 SOC of the battery storage for each solution

SOC	303 PV/0WG	252 PV/1WG	219 PV/2WGs	196 PV/3WGs
Above 80%	80.53%	86.01%	89.58%	92.58%
Above 50%	96.44%	96.69%	96.96%	98.94%
Below 30%	0.997%	1.081%	0.934%	0.347%
Below 10%	0.096%	0.097%	0.11%	0.074%

5.1.4 Varying the Capacity of the Battery Energy Storage. To study the effect of battery capacity on the $LCOE_U$, the battery energy storage is changed from 600 kWh to 1200 kWh. Figure 5.8 shows a comparison of $LCOE_U$ between each storage capacity using only PV modules.

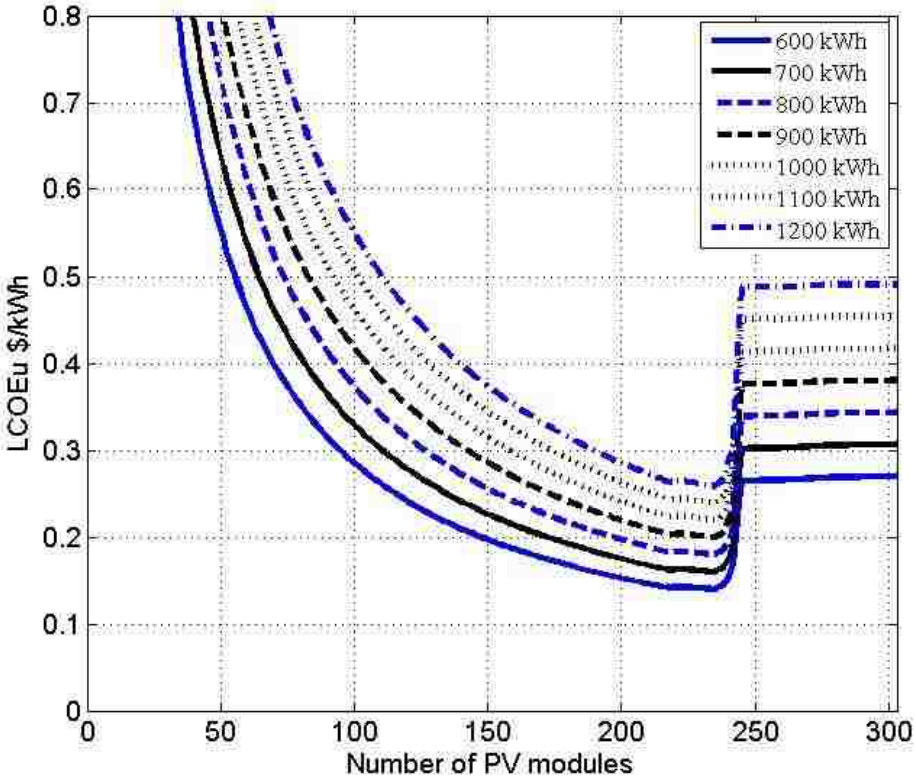

Figure 5.8 $LCOE_U$ at different storage capacity using only PV modules

Figure 5.9 is provided to show the effect of battery storage on the $LCOE_U$ and LCOEt at 100% availability. It is observed that the cost of energy increases as the capacity of battery storage increases for LCOE at utilized and unutilized EPG. Also, as the battery capacity increases, more energy is utilized and that reduces the rate at which the $LOCE_U$ increases with respect to the number of PV modules. Also, table 5.5 and table 5.6 show the numerical values of $LCOE_U$ and LCOEt versus the capacity of the battery energy storage with the corresponding numbers of PV modules and WGs. It is concluded

that the lowest $LCOE_U$ is 0.279 $/kWh when the battery capacity is the lowest with 439 PV modules and one wind generator. On the other hand, the lowest cost of LCOEt is 0.0384 $/kWh at 600 kWh battery capacity and 1425 PV modules. However, if there is a space limitation to this large number of PV modules, different combination is used.

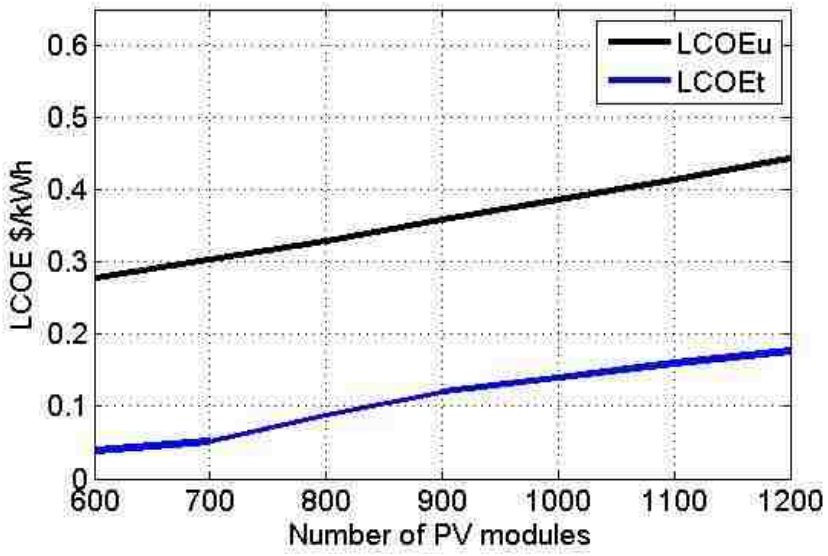

Figure 5.9 Effect of battery energy storage on LCOEt and LCOEu at 100% availability of power supply

Table 5.5 $LCOE_U$ of the PV/wind/battery energy MG system

Availability	100%						
Storage (kWh)	600	700	800	900	1000	1100	1200
number of PV modules	439	294	309	252	246	243	240
number of Wind Generators	1	2	1	2	2	2	2
$LCOE_U$($/kWh)	0.279	0.304	0.330	0.3586	0. 3868	0.4150	0.4434

Table 5.6 $LCOE_t$ of the PV/wind/battery energy MG system

Availability	100%						
Storage (kWh)	600	700	800	900	1000	1100	1200
number of PV modules	1425	961	522	397	369	347	337
number of Wind Generators	0	0	0	0	0	0	0
$LCOE_t$($/kWh)	0.0384	0.052	0.0874	0.12	0.1394	0.1597	0.1770

Moreover, the SOC of the battery storage for all solutions in table 5.6 are shown in figure 5.10, figure 5.11 (a, b), figure 5.12 (a, b), and figure 5.13.

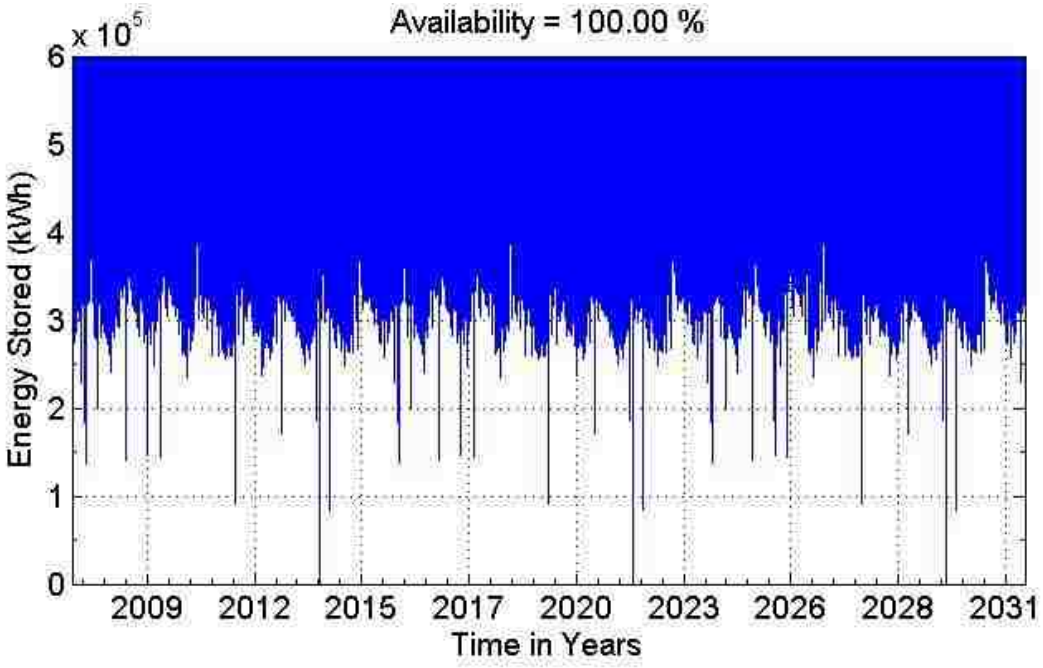

Figure 5.10 SOC of the battery storage throughout the system life cycle with 600kWh battery storage

(a)

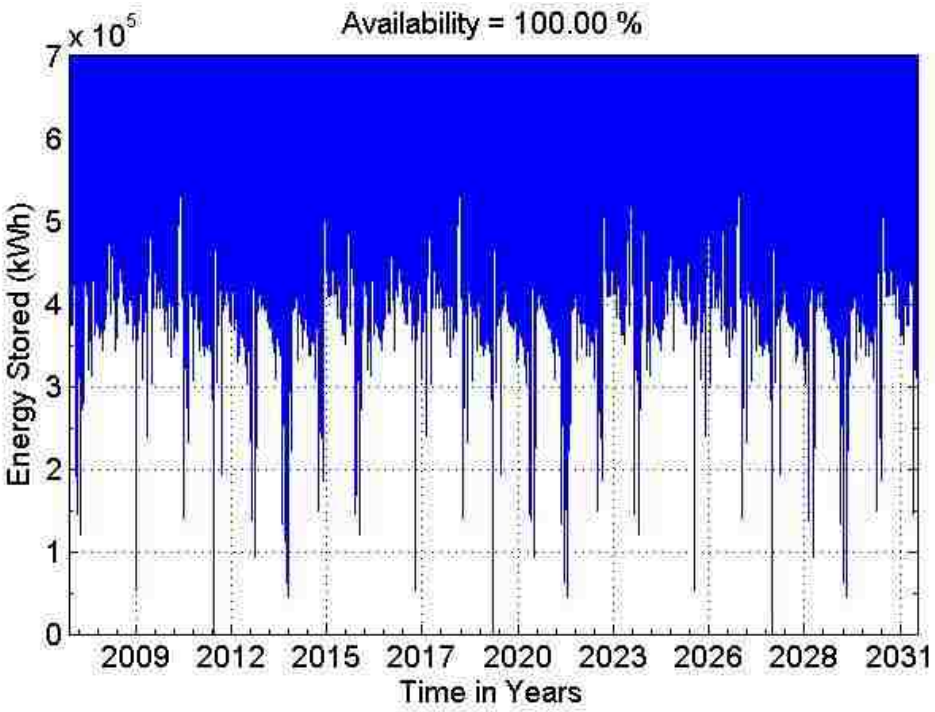

(b)

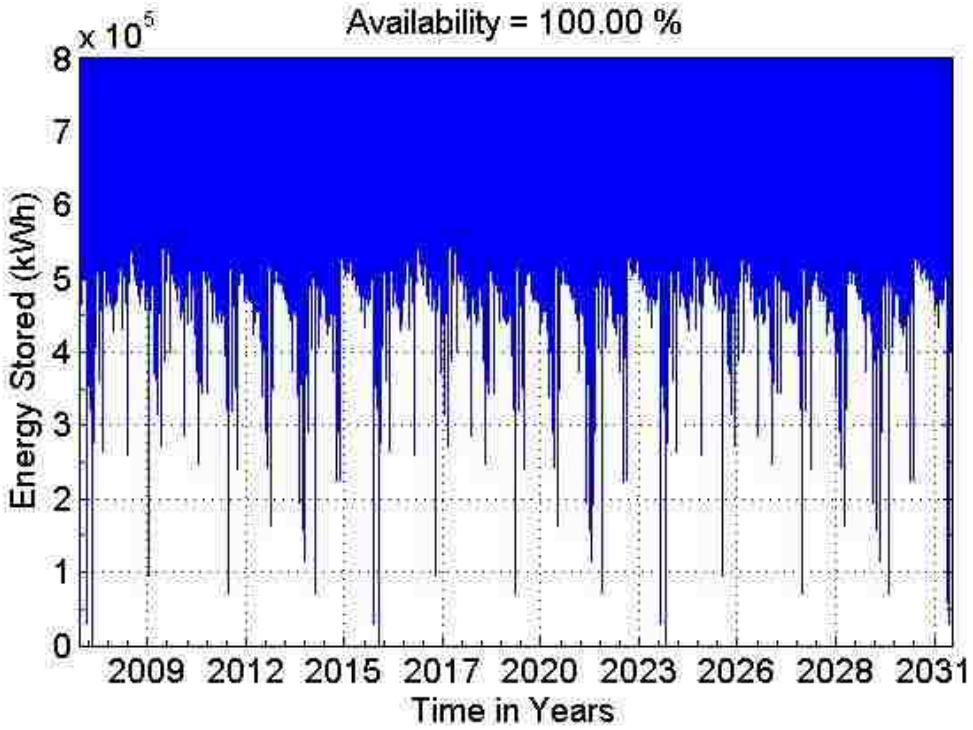

Figure 5.11 SOC of the battery storage throughout the system life cycle (a) 700 kWh (b) 800 kWh

a)

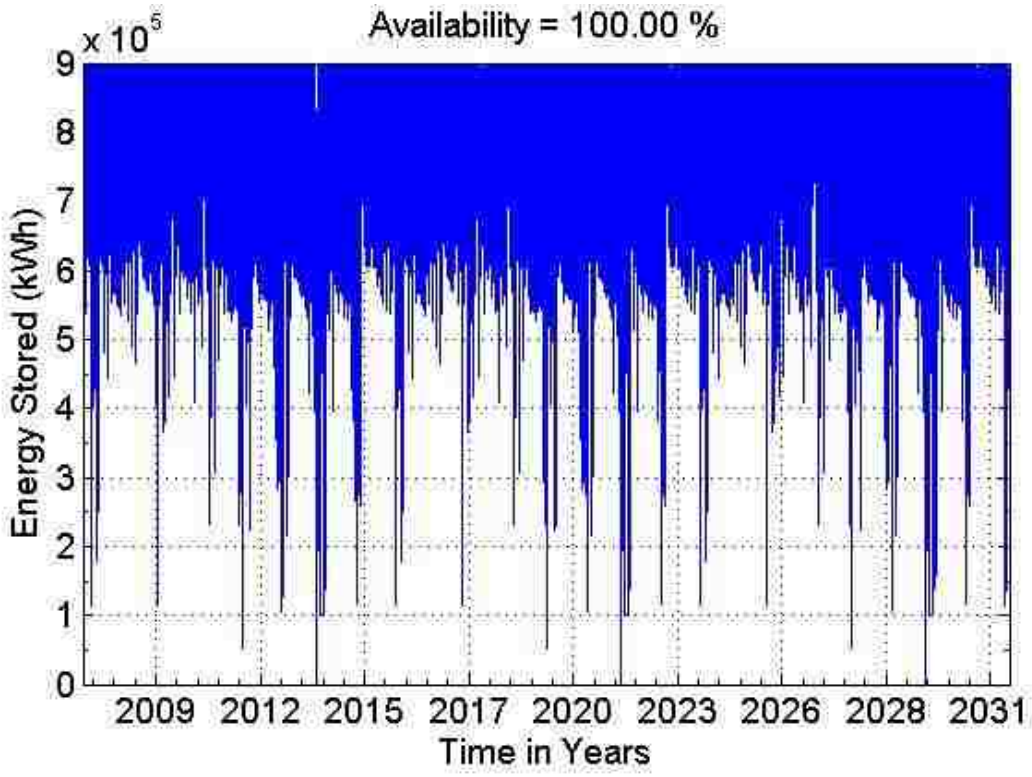

b)

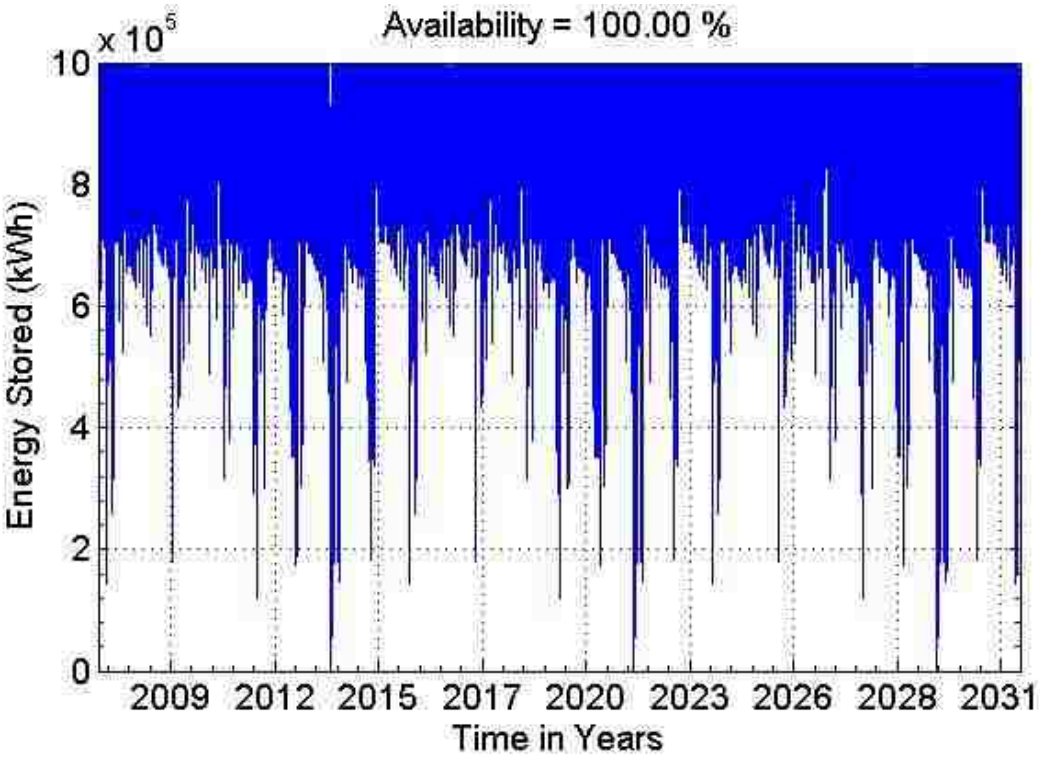

Figure 5.12 SOC of the battery storage throughout the system life cycle (a) 900kWh (b) 1000 kWh

a)

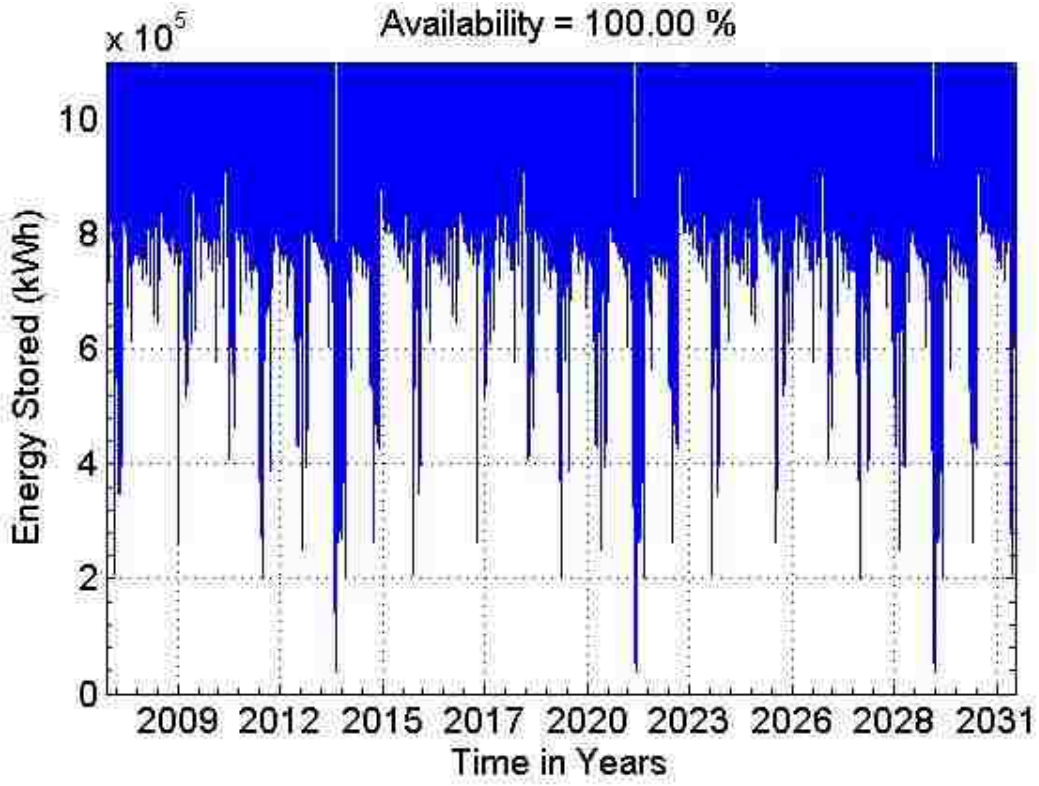

b)

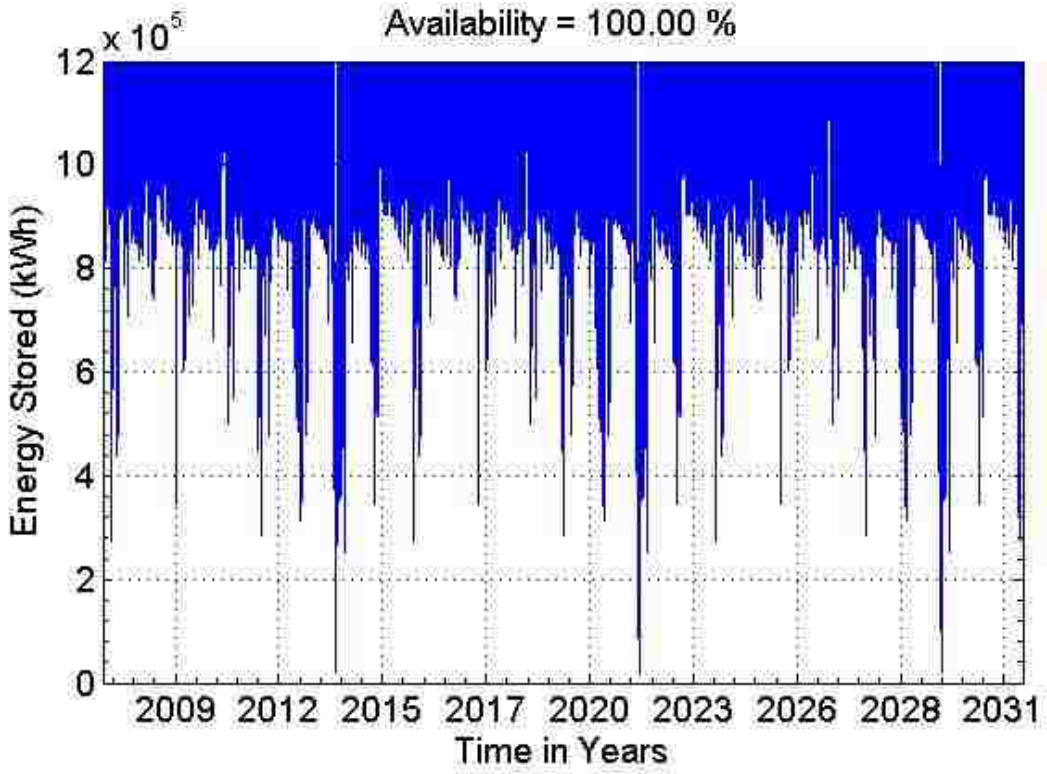

Figure 5.13 SOC of the battery storage throughout the system life cycle at (a) 1100 kWh (b) 1200 kWh

Now, the SOC of battery storage for each capacity is calculated and given in table 5.7 below. It can be observed that as the storage capacity increases, the percentage of the time the SOC of the battery is above 80% increases. As a result, the battery life will improve.

Table 5.7 SOC of each battery capacities throughout the system life cycle

SOC	600 kWh	700 kWh	800 kWh	900 kWh	1000 kWh	1100 kWh	1200 kWh
Above 80%	68.97%	75.1%	71.3%	77.61%	79.95%	82.57%	85.66%
Above 50%	98.5%	98.41%	98.18%	97.36%	97.38%	97.64%	97.83%
Below 30%	0.084%	0.358%	0.418%	0.73%	0.669%	0.505%	0.413%
Below 10%	0.001%	0.029%	0.005%	0.045%	0.045%	0.0036%	0.026%

5.1.5 Constant Load. So far, Forever Power method has been applied to a hybrid energy system with variable load. Now, we consider a constant load with 21 kW throughout the life cycle of the system. To compare the results of variable load a 600 kWh has been used. Figure 5.14 gives an example to show the difference in terms of availability between variable load and constant load. It can be observed that there is a very small difference for all combinations of the hybrid micro-sources.

The results of the LCOE is also found for constant load and compared to the LCOE for the variable load. The minimum $LCOE_U$ at 100 % availability is 0.2870 $/kWh at 430 PV modules and two WGs compared to 0.279 $/kWh for variable load. Also, the numbers of PV modules used decrease by around 9 modules for constant load while the number of WGs used increased by one. Thus, the $LCOE_U$ is higher for constant load than

for variable load with same annual energy demand and capacity of energy storage. However, there is a little improvement in the DOD cycles of the battery storage as shown in table 5.8.

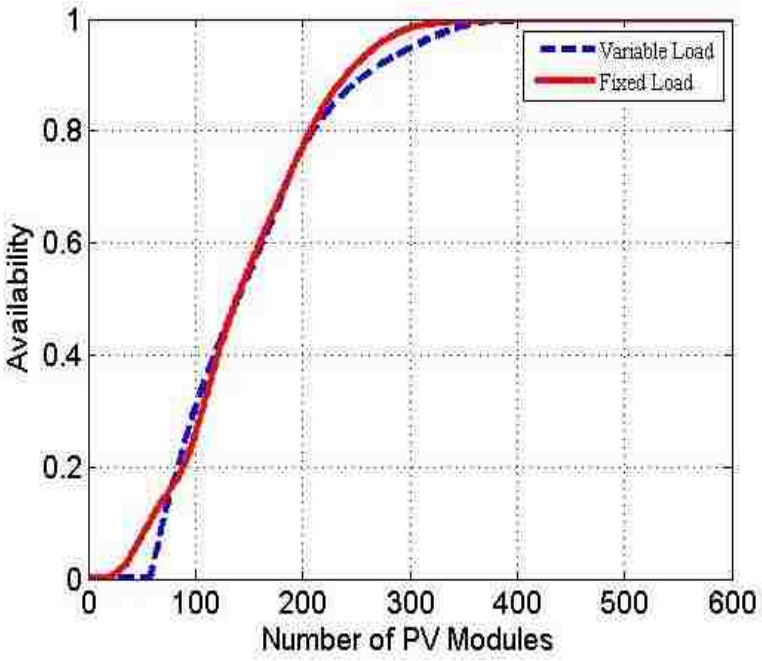

Figure 5.14 Availability of power at fixed and variable loads with only PV modules

Table 5.8 SOC of 600kWh battery storage for variable and constant loads

SOC	600 kWh	
	Variable load	Constant load
Above 80%	68.97%	71.89%
Above 50%	98.5%	99.69%
Below 30%	0.084%	0.042%
Below 10%	0.001%	0.008%

5.2 USING SMALLER WIND GENERATOR

To study the effect of the size of wind generator used on the LCOE, different sizes has been consider in this section as shown in table 5.9. Also, a 600 kWh of battery storage has been used.

Table 5.9 Effect of wind generator size on the $LCOE_U$

Availability	100%		
Battery capacity	600 kWh		
Wind generator size	25 kW	20 kW	10 kW
Number of Wind generators	1	2	5
$LCOE_U$ ($/kWh)	0.279	0.2910	0.2857

From table 5.9 we can conclude that there is a little effect of the size of wind generator on the cost of energy. The lowest $LCOE_U$ is 0.279 $/kWh which can be achieved by using a wind generator with rated power of 25 kW.

5.3 COMPARING TO HOMER PRO SOFTWARE

To study the effectiveness of this technique, it is compared to HOMER software. A one year wind, solar irradiance, temperature and load have been loaded into the program. The optimal solution, with one day storage and 0% LPSP, is shown in table 5.10. It is found that the $LCOE_U$ is 0.33 $/kWh which is higher than our results, 0.279 $/kWh, because the PV modules fade with time and are assumed to exhibit a power output of around 80% less of the minimum peak power after 25 years. Also, different

rating of wind generator is used in HOMER software since it does not have a 25 kW wind generator.

Table 5.10 Optimal solution

Power Source Type	HOMER Pro	Forever Power
Number of PV module (305 W)	495	439
Number of wind generators	1 (10 kW)	1 (25 kW)
Number of Battery units (1 kWh)	600	600
Initial capital cost ($)	514,900	585,253
NPC/LCC ($)	1,034,734	768,307
$LCOE_U$ ($/kWh)	0.33	0.279

5.4 UTILIZING EXCESS POWER GENERATION

To utilize the excess power generation from the PV and wind generators economically, it is better to use this energy than storing it. The proposed solution is to use the amount of excess power generation to supply power to a portable desalination unit at the proposed rural village in Saudi Arabia. The country is under extreme water shortages since there are no rivers or lakes [63]. Also, annual rainfall in Saudi Arabia is less than 100 mm [63]. The average cost of desalinated sea water is $0.8 per cubic meter while an average Saudi family only pays $2 per year with an average consumption of 260 liter per capita per day, which costs $0.208 to produce [63]. In this case study, it is assumed that the total demand for water is 5,000 liter per day, sufficient for 19-20 people. Table 5.11 shows the technical specification of the selected two desalination units for this village.

Each desalination unit is assumed to work only if the average EPG per hour is greater than 1500 watts.

Table 5.11 Desalination unit technical specification

Manufacturer	AMPAC USA, AP2200-LX
Capacity in liter per day	8330
Total power needed	~ 1500 Watt
Capacity per liter	240 liter per hour
Voltage	110 or 220 V, 1 phase
frequency	50 or 60 Hz
Capital Cost ($)	30,000
O&M ($)	300
Installation cost ($)	6000

The optimal solution of 439 PV modules, one WG and 600kWh battery storage is used. Two desalination units are used to supply water for the village. Once the EPG is greater than 3kW, each desalination unit will operate to produce 240 l/hr. Then, the total liters of water and utilized EPG are calculated throughout the system life. It is assumed that the desalination unit is replaced twice during the system life. After that the $LCOE_U$ is calculated again including the utilized amount of EPG. Table 5.12 shows the number of hours the desalination unit is operating for 25 years and the number of liters of distilled water generated. It can be observed that there is a negligible increase in $LCOE_U$ increases by 0.005 $/kWh. However, this cost can be considered as a combined cost of electricity and water which is a competitive price to what cost the government using conventional sources [63].

Table 5.12 using EPG to power two portable desalination units (for 25 years)

Number of desalination unit	2
Number of hours the desalination units operate	93,815 hours
EPG used	281,445 kWh
Average water per day	5346 liter per day
Updated $LCOE_U$	0.2845 $/kWh

6. CONCLUSION

In this thesis the Forever Power methodology has been developed to iteratively find the optimal size of PV/wind/battery hybrid energy system based on the availability of power supply and the lowest cost of energy. In this method, typical meteorological year data sets of hourly solar irradiance, temperature, and wind speed are needed to apply this method to a known electrical load. To verify the effectiveness of the methodology and the assumptions made, it was applied to a rural village near Yanbu city, Saudi Arabia. The village was assumed to have four homes with identical variable loads that have a combined average power of 21 kW. The battery storage was assumed to have four replacements throughout the system life cycle. This is justified since the DOD does not go below 50% for more than 97% of the time. Moreover, it was demonstrated that constant load profile can lead to almost similar $LCOE_U$ as for variable load with same average power. Also, it was observed that the size of the wind turbine has negligible effect on the $LCOE_U$. On the other hand, the battery capacity has a large effect on the $LCOE_U$. It is recommended to start the iteration with one day storage and increment up to three days storage for the hybrid MG system. The optimal solution on this particular case study was found to be 0.279 $/kWh which is higher than what cost from utility, 0.2133 $/kWh, before government subsidies. However, after utilizing EPG to power two desalination units to cover water demand by the village the combined cost of electricity and water is 0.281 $/kWh which is lower than the combined cost of water and electricity from utility [63]. It is recommended that government of Saudi Arabia need to use wind and solar hybrid energy system to electrify rural villages and provide water supply instead of using diesel generators for economic and environmental benefits.

In this thesis, simplified model of PV, wind and battery energy storage have been used. It is better to have more accurate model for the PV array that includes tilt angle effect on PV model. Also, a more accurate model for wind generator to include swept area will be considered. Moreover, accurate model for the battery energy storage that includes temperature effect on the capacity is going to be used. Finally, fading of PV module and battery capacity will be included in the iteration.

REFERENCES

[1] U.S. Energy Information Administration (EIA), 'Saudi Arabia - Analysis - U.S. Energy Information Administration (EIA)', 2015. [Online]. Available: http://www.eia.gov/countries/cab.cfm?fips=SA. [Accessed: 20- Feb- 2015].

[2] Middle East Economic Survey, "Saudi Arabia in Power Generation Efficiency Drive" (April 4, 2014), page 8.

[3] A. Alshehry and M. Belloumi, 'Energy consumption, carbon dioxide emissions and economic growth: The case of Saudi Arabia', *Renewable and Sustainable Energy Reviews*, vol. 41, pp. 237-247, 2015.

[4] Saudi Electricity Company, 'Saudi Electricity Company Annual Report 2013', 2014. [Online]. Available: https://www.se.com.sa/en-us/Pages/AnnualReports.aspx. [Accessed: 03- Feb- 2015].

[5] Middle East Economic Survey, "KACARE Outlines Saudi Electricity Energy Source Scenario" (May 3, 2013), page 7.

[6] Alghanim. M.H, Mallick. P.K,“ Utilization of Smart Grid and Renewable Energy toward a Sustainable Future in Saudi Arabia.” International Conference on Renewable Energies and Power Quality (ICREPQ’15), March, 2015.

[7] Saudi Arabia energy efficiency report, ABB global, April, 2012. (Online, 2015)

[8] The Electricity & Cogeneration Regulatory Authority (ECRA) 'Activities and Achievements of the Authority 2013', 2014. [Online]. Available: http://www.ecra.gov.sa/reports.aspx. [Accessed: 05- Feb- 2015].

[9] I. Mahtab, 'Global Markets: Solar in Saudi Arabia', Saudi Arabia Solar Industry Association, 2014.

[10] The Electricity & Cogeneration Regulatory Authority (ECRA) 'Activities and Achievements of the Authority 2013', 2014. [Online]. Available: http://www.ecra.gov.sa/reports.aspx. [Accessed: 05- Feb- 2015].

[11] Ecra.gov.sa, 'The electricity & cogeneration Regulatory Authority', 2015. [Online]. Available: http://www.ecra.gov.sa/home.aspx. [Accessed: 07- Mar- 2015].

[12] Middle East Economic Survey, "KACARE Outlines Saudi Electricity Energy Source Scenario" (May 3, 2013), page 7

[13] Deaves, M. "Solar achieves grid parity in Saudi Arabia – Significant developments expected", ClearSky Advisors, Feb. 2015 [online]

[14] S. Rehman, M. Bader and S. Al-Moallem, 'Cost of solar energy generated using PV panels',*Renewable and Sustainable Energy Reviews*, vol. 11, no. 8, pp. 1843-1857, 2007.

[15] A. Almasoud and H. Gandayh, 'Future of solar energy in Saudi Arabia', *Journal of King Saud University - Engineering Sciences*, vol. 27, no. 2, pp. 153-157, 2015.

[16] State University of New York/ Albany, March 1999 – February 2013; DeLorme World Base Map 2010, DeLorme Publishing Company. Inc.

[17] S. Alawaji, 'Evaluation of solar energy research and its applications in Saudi Arabia — 20 years of experience', *Renewable and Sustainable Energy Reviews*, vol. 5, no. 1, pp. 59-77, 2001.

[18] M. Amin and M. El-Samanoudy, 'Feasibility study of wind energy utilization in Saudi Arabia',*Journal of Wind Engineering and Industrial Aerodynamics*, vol. 18, no. 2, pp. 153-163, 1985.

[19] Ansari J, Madni IK, Bakhsh H. Saudi Arabian wind energy atlas. Riyadh, Saudi Arabia: KACST; 1986, p. 1-27.

[20] S. Rehman, T. Halawani and T. Husain, 'Weibull parameters for wind speed distribution in Saudi Arabia', *Solar Energy*, vol. 53, no. 6, pp. 473-479, 1994.

[21] S. Rehman, T. Halawani and M. Mohandes, 'Wind power cost assessment at twenty locations in the kingdom of Saudi Arabia', *Renewable Energy*, vol. 28, no. 4, pp. 573-583, 2003.

[22] Said SAM, El-Amin IM, Al-Shehri AM. Renewable energy potentials in Saudi Arabia. In: Beirut regional collaboration workshop on energy efficiency and renewable energy technology. American University of Beirut; April 2004. p.76-82.

[23] S. Rehman, 'Prospects of wind farm development in Saudi Arabia', *Renewable Energy*, vol. 30, no. 3, pp. 447-463, 2005.

[24] Rahman F, Rehman S, Arif M, Majeed A., "Overview of energy storage systems for storing electricity from renewable energy sources in Saudi Arabia." Renew Sustain Energy Rev, Vol. 16, pp.274–283, 2012.

[25] International Energy Agency, 'World Energy Outlook 2014', 2015. [Online]. Available: http://www.worldenergyoutlook.org/resources/energydevelopment/. [Accessed: 06- Apr- 2015].

[26] The Department of Energy, "Summary Report: 2012 DOE Microgrid Workshop," DOE EERE, Chicago, 2012.

[27] T. Glenwright, "http://www.smartgrid-live.com/wp-content/uploads/2012/12/Introduction to-Microgrids-by-Tristan-Glenwright.pdf.," December 2012. [Online].

[28] R. Luna-Rubio, M. Trejo-Perea, D. Vargas-Vázquez and G. Ríos-Moreno, 'Optimal sizing of renewable hybrids energy systems: A review of methodologies', *Solar Energy*, vol. 86, no. 4, pp. 1077-1088, 2012.

[29] A. Chauhan and R. Saini, 'A review on Integrated Renewable Energy System based power generation for stand-alone applications: Configurations, storage options, sizing methodologies and control', *Renewable and Sustainable Energy Reviews*, vol. 38, pp. 99-120, 2014.

[30] S. Diaf, M. Belhamel, M. Haddadi and A. Louche, 'Technical and economic assessment of hybrid photovoltaic/wind system with battery storage in Corsica island', *Energy Policy*, vol. 36, no. 2, pp. 743-754, 2008.

[31] A. Prasad and E. Natarajan, 'Optimization of integrated photovoltaic–wind power generation systems with battery storage', *Energy*, vol. 31, no. 12, pp. 1943-1954, 2006.

[32] H. Yang, L. Lu and W. Zhou, 'A novel optimization sizing model for hybrid solar-wind power generation system', *Solar Energy*, vol. 81, no. 1, pp. 76-84, 2007.

[33] H. Yang, W. Zhou, L. Lu and Z. Fang, 'Optimal sizing method for stand-alone hybrid solar–wind system with LPSP technology by using genetic algorithm', *Solar Energy*, vol. 82, no. 4, pp. 354-367, 2008.

[34] Hongxing Yang , Lin Lu, Wei Zhou. A novel optimization sizing model for hybrid solar-wind power generation system, Solar Energy 81 (2007) 76–84.

[35] A. Askarzadeh, 'A discrete chaotic harmony search-based simulated annealing algorithm for optimum design of PV/wind hybrid system', *Solar Energy*, vol. 97, pp. 93-101, 2013.

[36] R. Kumar, R. Gupta and A. Bansal, 'Economic analysis and power management of a stand-alone wind/photovoltaic hybrid energy system using biogeography based optimization algorithm', *Swarm and Evolutionary Computation*, vol. 8, pp. 33-43, 2013.

[37] O. Ekren and B. Ekren, 'Size optimization of a PV/wind hybrid energy conversion system with battery storage using response surface methodology', *Applied Energy*, vol. 85, no. 11, pp. 1086-1101, 2008.

[38] A. Arabali, M. Ghofrani, M. Etezadi-Amoli, M. Fadali and Y. Baghzouz, 'Genetic-Algorithm-Based Optimization Approach for Energy Management', *IEEE Trans. Power Delivery*, vol. 28, no. 1, pp. 162-170, 2013.

[39] A. Kashefi Kaviani, G. Riahy and S. Kouhsari, 'Optimal design of a reliable hydrogen-based stand-alone wind/PV generating system, considering component outages', *Renewable Energy*, vol. 34, no. 11, pp. 2380-2390, 2009.

[40] Y. Katsigiannis, P. Georgilakis and E. Karapidakis, 'Multiobjective genetic algorithm solution to the optimum economic and environmental performance problem of small autonomous hybrid power systems with renewables', *IET Renew. Power Gener.*, vol. 4, no. 5, p. 404, 2010.

[41] P. Moura and A. de Almeida, 'Multi-objective optimization of a mixed renewable system with demand-side management', *Renewable and Sustainable Energy Reviews*, vol. 14, no. 5, pp. 1461-1468, 2010.

[42] B. Ould Bilal, V. Sambou, P. Ndiaye, C. Kébé and M. Ndongo, 'Optimal design of a hybrid solar–wind-battery system using the minimization of the annualized cost system and the minimization of the loss of power supply probability (LPSP)', *Renewable Energy*, vol. 35, no. 10, pp. 2388-2390, 2010.

[43] D. Abbes, A. Martinez and G. Champenois, 'Life cycle cost, embodied energy and loss of power supply probability for the optimal design of hybrid power systems', *Mathematics and Computers in Simulation*, vol. 98, pp. 46-62, 2014.

[44] S. Karaki, R. Chedid and R. Ramadan, 'Probabilistic performance assessment of autonomous solar-wind energy conversion systems', *IEEE Trans. On energy Conversion*, vol. 14, no. 3, pp. 766-772, 1999.

[45] H. Yang, L. Lu and J. Burnett, 'Weather data and probability analysis of hybrid photovoltaic–wind power generation systems in Hong Kong', *Renewable Energy*, vol. 28, no. 11, pp. 1813-1824, 2003.

[46] G. Tina and S. Gagliano, 'Probabilistic analysis of weather data for a hybrid solar/wind energy system', *International Journal of Energy Research*, vol. 35, no. 3, pp. 221-232, 2011.

[47] G. Tina, S. Gagliano and S. Raiti, 'Hybrid solar/wind power system probabilistic modelling for long-term performance assessment', *Solar Energy*, vol. 80, no. 5, pp. 578-588, 2006.

[48] D. Khatod, V. Pant and J. Sharma, 'Analytical Approach for Well-Being Assessment of Small Autonomous Power Systems With Solar and Wind Energy Sources', *IEEE Transactions on Energy Conversion*, vol. 25, no. 2, pp. 535-545, 2010.

[49] N. Mohammad, M. Quamruzzaman, M. Hossain and M. Alam, 'Parasitic Effects on the Performance of DC-DC SEPIC in Photovoltaic Maximum Power Point Tracking Applications', *SGRE*, vol. 04, no. 01, pp. 113-121, 2013.

[50] R. Francisco and D. Cruz, 'An Optimized Maximum Power Point Tracking Method Based on PV Surface Temperature Measurement', *Sustainable Energy - Recent Studies*, 2012.

[51] National Instruments, “Wind Turbine Control Methods.” Published: Dec, 03,2008, available online: http://www.ni.com/white-paper/8189/en/

[52] J. Tester, *Sustainable energy*. Cambridge, Mass.: MIT Press, 2005.

[53] A. Ernesto, M. Gustavo and P. Enrique, 'Dynamic Modelling of Advanced Battery Energy Storage System for Grid-Tied AC Microgrid Applications', *Energy Storage - Technologies and Applications*, 2013.

[54] H. Zhao, Q. Wu, S. Hu, H. Xu and C. Rasmussen, 'Review of energy storage system for wind power integration support', *Applied Energy*, vol. 137, pp. 545-553, 2015.

[55] X. Luo, J. Wang, M. Dooner and J. Clarke, 'Overview of current development in electrical energy storage technologies and the application potential in power system operation', *Applied Energy*, vol. 137, pp. 511-536, 2015.

[56] James J. Kauzlarich, “Wheelchair batteries II: Capacity, sizing, and life” Journal of Rehabilitation Research and Development Vol . 27 No. 2, 1990 Pages 163-170.

[57] U.S. Battery, Leader in Deep Cycle Batteries, 'Expected Cycle Life vs. DOD', 2014. [Online]. Available: http://usbattery.com/. [Accessed: 13- May- 2015].

[58] E. Hittinger, T. Wiley, J. Kluza and J. Whitacre, 'Evaluating the value of batteries in microgrid electricity systems using an improved Energy Systems Model', *Energy Conversion and Management*, vol. 89, pp. 458-472, 2015.

[59] R. Dufo-López, J. Lujano-Rojas and J. Bernal-Agustín, 'Comparison of different lead–acid battery lifetime prediction models for use in simulation of stand-alone photovoltaic systems', *Applied Energy*, vol. 115, pp. 242-253, 2014.

[60] J. Kimball, B. Kuhn and R. Balog, 'A System Design Approach for Unattended Solar Energy Harvesting Supply', *IEEE Transactions on Power Electronics*, vol. 24, no. 4, pp. 952-962, 2009.

[61] T. Johansson and L. Burnham, *Renewable energy*. Washington, D.C.: Island Press, 1993.

[62] A. Alaidroos and L. He, 'Feasibility Of Renewable Energy Based Distributed Generations In Yanbu, Saudi Arabia', *Oxford Abstracts: American Solar Energy Society*, 2012. [Online]. Available: https://ases.conference-services.net. [Accessed: 10- Oct- 2014].

[63] Ouda. Omar, "Towards Assessment of Saudi Arabia Public Awareness of Water Shortage Problem." Resources and Environment, vol. 3.pp.10-13, 2013.

VITA

Sami Hamed Alalwani was born on March 13, 1985 at Yanbu, Saudi Arabia. His high school education was completed in Haneen High school, Yanbu, Saudi Arabia. He received his Bachelor of Science degree in Electrical Engineering Technology from Yanbu Industrial College, Yanbu, Saudi Arabia in April 2011. In June of 2011, Sami joined Royal Commission of Yanbu Colleges and Institutes as an instructor in the Electrical power engineering technology department. In August 2013, he began his Master of Science program in Electrical Engineering at Missouri University of Science and Technology. He obtained his Master's degree in August, 2015.